

On the role of relaxation and acceleration in the non-overlapping Schwarz alternating method for coupling

Giulia Sambataro^{a,*}, Irina Tezaur^b

^a*Université de Strasbourg, CNRS, Inria, IRMA, 7 rue René-Descartes, Strasbourg Cedex, 67084, France*

^b*Sandia National Laboratories, 7011 East Ave, Livermore, 94550, CA, United States*

Abstract

The purpose of this paper is to study the influence of relaxation and acceleration techniques on the convergence behavior of the non-overlapping Schwarz algorithm with alternating Dirichlet-Neumann transmission conditions in the context of domain decomposition- (DD-) based coupling. After demonstrating that the multiplicative Schwarz scheme can be formulated as a fixed-point iteration, we explore, both theoretically and numerically, two promising techniques for speeding up the method: (i) Aitken acceleration and (ii) Anderson acceleration. In the process, we derive a robust and efficient adaptive variant of Anderson acceleration, termed “Anderson with memory adaptation”. We compare the proposed acceleration strategies to the well-known classical relaxed Dirichlet-Neumann Schwarz alternating method. Our results suggest that, while Aitken-accelerated Schwarz is the best approach in terms of efficiency and robustness when considering two sub-domain DDs, Anderson-accelerated Schwarz is the method of choice in larger multi-domain settings.

Keywords: Non-overlapping domain decomposition, Dirichlet-Neumann Schwarz algorithm, relaxation, Aitken acceleration, Anderson acceleration, fixed-point iteration, nonlinear elasticity.

*Corresponding author. Email: giulia.sambataro@inria.fr

1. Introduction

Domain decomposition (DD) methods have become a fundamental tool for the numerical solution of large-scale partial differential equations (PDEs)¹. A popular DD-based approach is the Schwarz alternating method, which is particularly attractive for parallel computing, as it: (i) requires only sub-domain-local solves, (ii) performs local communications between neighboring sub-domains to exchange boundary condition (BC) information at sub-domain interfaces, and (iii) can be implemented in a minimally-intrusive way into existing high-performance computing codes. While the Schwarz alternating method is most commonly known in the linear solver literature, where it is often used as a preconditioner that can accelerate the convergence of Krylov iterative solvers [2], several recent works [3, 4, 5, 6, 7, 8] have shown that the method can also be used as a concurrent multiscale coupling method capable of stitching together regions with different mesh resolutions, different element types, different time integration schemes (e.g., implicit and explicit [4, 8]) and different models (e.g., finite element and data-driven models [5, 6, 9, 7, 8]), all without introducing any artifacts exhibited by alternative coupling methods.

The Schwarz alternating method can be applied in the context of both overlapping and non-overlapping DDs, each with their own inherent advantages and disadvantages: whereas the overlapping Schwarz variant has more favorable convergence properties, the non-overlapping Schwarz scheme is more flexible, making it particularly attractive for multi-physics and multi-material applications because it allows completely independent meshing of the coupled sub-domains [4, 8]. A number of authors, including Schwarz himself [10], have studied the theoretical properties of the overlapping Schwarz alternating method [11, 12, 13], demonstrating convergence with Dirichlet-Dirichlet transmission conditions provided that the overlap region is non-empty. Extensions to the case of non-overlapping DDs were made concurrently by Lions [14] and Zanolli *et al.* [15, 16], who showed that either Robin-Robin or alternating Dirichlet-Neumann transmission conditions can yield a provably convergent algorithm. These foundational contributions paved the way for later developments, e.g., the so-called non-overlapping Schwarz wave-

¹A nice overview of DD methods, including both overlapping and non-overlapping approaches, is provided by Nataf in [1], which offers an accessible yet thorough introduction to these methods, with a particular emphasis on their applications to PDEs.

form relaxation method, particularly relevant for time-dependent problems, in which a Dirichlet-Dirichlet iteration in both sub-domains is followed by a Neumann-Neumann iteration [17, 18, 19].

The present work is concerned with the non-overlapping variant of the Schwarz alternating method as a mechanism to perform flexible concurrent DD-based coupling in the context of PDE-based modeling and simulation (mod/sim) of scenarios where overlapping DD-based methods are not feasible. A well-known disadvantage of non-overlapping Schwarz is the fact that it is slower and less robust than overlapping Schwarz, often requiring more iterations to reach convergence or not converging at all. This is especially problematic for PDEs with highly heterogeneous coefficients, discretized using fine meshes, and/or posed on long and thin sub-domains [20].

To mitigate the non-overlapping Schwarz convergence issues described above, various authors have explored acceleration strategies and algorithmic improvements for non-overlapping alternating Schwarz-based DD methods. The so-called optimized Schwarz methods define a well-known class of accelerated Schwarz techniques based on the Robin-Robin formulation [14], in which optimal values of the parameters pre-multiplying the Dirichlet and Neumann parts of the Robin BCs are derived [2]. The main disadvantage of these approaches is that the optimal parameter values are generally problem-specific and require lengthy analytical derivations. Within the alternating Dirichlet-Neumann Schwarz framework, it has been shown that convergence can be accelerated through the addition of a relaxation step to the Dirichlet sub-problem [21]. Although several authors, e.g., [22] and [17], have investigated automatic strategies for choosing the relaxation parameter, the method is not particularly robust with respect to the choice of this parameter; moreover, the optimal value of this parameter is often very problem- and DD-specific.

The present work explores and analyzes both numerically and theoretically two alternative approaches for accelerating the Dirichlet-Neumann form of the non-overlapping Schwarz alternating method: Aitken [23] and Anderson [24] acceleration. We choose to focus on the Dirichlet-Neumann (rather than the Robin-Robin) variant of Schwarz, as Dirichlet and Neumann conditions are more readily available in physics-based PDE codes; for example, all solid mechanics codes come equipped with Neumann (traction) BCs, whereas Robin BCs are generally not used within this domain, as they do not have a physical interpretation. Since Aitken and Anderson acceleration are designed for speeding up solvers based on fixed-point iterations, applying these methods to Schwarz requires rewriting the classical Schwarz algorithm as a

fixed-point iteration. To the authors’ knowledge, the earliest reference that considers an Aitken-accelerated Schwarz method is [25]; however, like most references on this topic, e.g., [26], attention is restricted to the overlapping DD case. Prior attempts to speed up Schwarz using Anderson acceleration, e.g., [24], have also focused on the overlapping variant of this method. Within the non-overlapping DD setting, Aitken acceleration has been shown as a valid alternative for accelerating the Schwarz algorithm in the context of fluid-structure interaction problems in [27]. We are not aware of references that attempt to apply Anderson acceleration to non-overlapping Schwarz. We are also not aware of publications that perform a systematic comparison of classical relaxation, Aitken acceleration and Anderson acceleration as mechanisms to speed up the non-overlapping Schwarz algorithm.

Toward this effect, the main novel contributions of this work are as follows: (i) the first (to our knowledge) adaptation of Anderson acceleration to the non-overlapping Dirichlet-Neumann Schwarz alternating method and in particular, the development of an adaptive variant, termed “Anderson with memory adaptation”, which gives rise to a more robust and efficient Schwarz scheme (see Section 2); (ii) some theoretical analyses of Aitken-accelerated and Anderson-accelerated non-overlapping Dirichlet-Neumann Schwarz alternating method applied to a one-dimensional (1D) study case (see Section 2); and (iii) numerical studies comparing Aitken-accelerated and Anderson-accelerated Schwarz to Schwarz with classical relaxation, which verify numerically the theoretical properties derived herein on problems with DDs consisting of as many as five sub-domains (see Section 3). Conclusions and some avenues for future work are discussed in Section 4, after the main exposition.

2. Non-overlapping Schwarz for DD-based coupling

2.1. Problem formulation

We begin by introducing our non-overlapping DD notation. We consider a domain $\Omega \subset \mathbb{R}^d$ with Lipschitz boundary $\partial\Omega$ and $x \in \bar{\Omega}$ a space variable; in the present work, attention is restricted to the case when $d = 2$ (Figure 1(a)). Let $\mathcal{X} = [H_0^1(\Omega)]^d$ denote a Hilbert space endowed with the norm $\|v\|_{\mathcal{X}} := \|v\|_{H^1(\Omega)}$. Consider a generic elliptic PDE with variational form

$$\mathcal{R}(u, v) = 0 \quad \forall v \in \mathcal{X}, \tag{1}$$

where $\mathcal{R}(\cdot, \cdot)$ is a generic nonlinear operator. We assume that the problem (1) is well-posed and has a unique solution. Let \mathbf{n} denote the outward unit normal on $\partial\Omega$.

Suppose we are given a non-overlapping decomposition of Ω into N_{dd} open sub-domains $\{\Omega_i\}_{i=1}^{N_{\text{dd}}}$ such that

$$\Omega = \bigcup_{i=1}^{N_{\text{dd}}} \bar{\Omega}_i, \quad \Omega_i \cap \Omega_j = \emptyset \quad \text{for } i \neq j.$$

Without loss of generality, we will assume in the majority of our presentation that $N_{\text{dd}} = 2$, that is, the domain Ω is decomposed into two non-overlapping sub-domains, as shown in Figure 1(b)². The interface that separates the two sub-domains is denoted by Γ , so that $\Gamma := \bar{\Omega}_1 \cap \bar{\Omega}_2$. We assume that the boundaries Γ , $\partial\Omega_1 \setminus \Gamma$ and $\partial\Omega_2 \setminus \Gamma$ all have a non-vanishing $(d-1)$ -dimensional measure. The vectors \mathbf{n}_i , $i = 1, 2$, are the unit outward normals of Ω_i on Γ , so that $\mathbf{n}_1 = -\mathbf{n}_2$. The normal derivative is denoted by $\frac{\partial u}{\partial \mathbf{n}} = \nabla u \cdot \mathbf{n} \in H^{-1/2}(\Gamma)$. We denote the external boundaries, also referred to as the system boundaries, by $\partial\Omega_i^e = \partial\Omega_i \cap \partial\Omega$ for $i = 1, \dots, N_{\text{dd}}$.

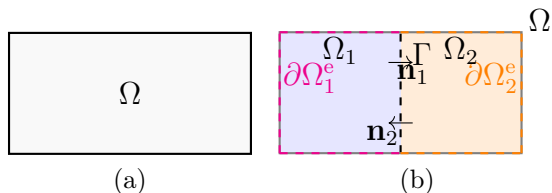


Figure 1: (a) Global domain. (b) Sketch of a non-overlapping decomposition of the domain Ω into Ω_1 and Ω_2 with interface Γ .

After introducing the following spaces

$$\mathcal{X}_i = \{v|_{\Omega_i}, v \in \mathcal{X}\} = [H^1(\Omega_i)]^d, \quad \mathcal{X}_{i,0} = \{v \in \mathcal{X}_i \mid v = 0 \text{ at } \Gamma_{i,\text{dir}}\}, \quad (2)$$

(where $\Gamma_{i,\text{dir}} \subset \partial\Omega_i$ is the local boundary associated with Dirichlet boundary conditions for subdomain Ω_i), the local sub-problems corresponding to the global problem (1) can be written in variational form as follows:

$$\mathcal{R}_i(u_i, v) = 0 \quad \forall v \in \mathcal{X}_{i,0}, \quad (3)$$

²Note that the $N_{\text{dd}} > 2$ case is explored numerically in Section 3.2.6.

where $\mathcal{R}_i : \mathcal{X}_i \rightarrow \mathbb{R}$ is the restriction of the global operator \mathcal{R} to Ω_i . We equip the local Hilbert spaces \mathcal{X}_i with the norms $\|v\|_{\mathcal{X}_i} = \|v\|_{H^1(\Omega_i)}$ for $i = 1, \dots, N_{\text{dd}}$. Herein, we will consider finite element (FE) discretizations of the global and local domains. Within this context, let $\mathcal{V} \subset \mathcal{X}$ and $\mathcal{V}_i \subset \mathcal{X}_i$ denote the discrete global and local FE spaces, respectively, and assume that each sub-domain discretization is based on nodal FE bases $\{\boldsymbol{\varphi}_i^j\}_{j=1}^{N_i}$. The discrete finite element spaces can now be expressed as $\mathcal{V}_i = \text{span}\{\boldsymbol{\varphi}_i^j\}_{j=1}^{N_i}$, where N_i is the number of nodes in the i^{th} sub-domain.

One advantage of the Schwarz alternating method for coupling is that it allows the sub-domains Ω_i to be discretized by different non-conformal meshes (c.f., [28, 29]). Consequently, each sub-domain can maintain a distinct discrete representation of the shared interface. We therefore introduce the notation Γ_{ij} to denote the discrete representation of Γ that conforms to the local mesh of Ω_i .

Let $\mathcal{U}_i = \{v|_{\Gamma_{ij}} : v \in \mathcal{V}_i\} \subset H^{1/2}(\Gamma_{ij})$ denote the discrete trace, defined as the restriction of the FE space \mathcal{V}_i to the local interface Γ_{ij} . We denote the standard discrete trace operator onto this space by $\gamma_i : \mathcal{V}_i \rightarrow \mathcal{U}_i$ for $i = 1, \dots, N_{\text{dd}}$. To adapt the notation to non-conforming interfaces, we also introduce the composition operator $\gamma_j^i : \mathcal{V}_j \rightarrow \mathcal{U}_i$ such that $\gamma_j^i(\mathbf{u}_j) = \Pi_{ij} \circ \gamma_j(\mathbf{u}_j)$, where the projection operator $\Pi_{ij} : \mathcal{U}_j \rightarrow \mathcal{U}_i$ is used to compute the trace of the solution \mathbf{u}_j on the interface Γ_{ij} of sub-domain Ω_i . Finally, we introduce the discrete Neumann operator $\Psi_i : \mathcal{V}_i \rightarrow \mathcal{U}_i^*$, which evaluates the discrete normal derivative on the interface Γ_{ij} . Acting as the discrete counterpart to the continuous normal trace $\partial_{\mathbf{n}_i} u_i \in H^{-1/2}(\Gamma_{ij})$, the operator Ψ_i is defined in a weak sense and takes values in \mathcal{U}_i^* , the formal dual space of \mathcal{U}_i .

2.2. Dirichlet-Neumann Schwarz scheme

Herein, we overview the classical Dirichlet-Neumann version of the non-overlapping Schwarz alternating method. We describe the algorithm for the simple case $N_{\text{dd}} = 2$, as shown in Figure 1(b). The solution to the global problem (1) on Ω is obtained via an iterative process in which a sequence of sub-domain-local problems is solved, with information propagating between sub-domains through transmission BCs. Algorithm 1 summarizes this procedure. Let the maximum number of iterations $\text{maxit} \in \mathbb{N}_0$ be given, as well as tolerances $\epsilon_{\text{abs}} > 0$ and $\epsilon_{\text{rel}} > 0$. We define the discrete residual operator $\mathcal{R}_i^h : \mathcal{V}_i \times \mathcal{V}_i \rightarrow \mathbb{R}$ as the restriction of the continuous residual operator \mathcal{R}_i

(3) to the discrete spaces \mathcal{V}_i . For simplicity of notation, we will drop the superscript h from this point forward, so that $\mathcal{R}_i(\mathbf{u}_i^{(k)}, \mathbf{v})$ denotes the discrete residual computed at Schwarz iteration k (c.f., (3)). The Schwarz iteration process requires an initial value of the interface trace at Γ_{21} , i.e., $\gamma_2(\mathbf{u}_2) \in \mathcal{U}_2$, which we denote as $\mathbf{g}^{(1)}$, where the superscript points out the fact that these data are used at the first iteration $k = 1$.

Remark 1. As clear from (2), the space $\mathcal{X}_{i,0}$ incorporates homogeneous Dirichlet BCs on the external boundary $\partial\Omega_i^e$, meaning they can be imposed strongly by defining the trial space \mathcal{X}_i . Neumann BCs are accounted for through the residual operator \mathcal{R}_i . Thus, in Algorithm 1, only interface BCs are explicitly written.

Algorithm 1 Dirichlet–Neumann scheme with relaxation.

Require: Initial guess $\mathbf{g}^{(1)}$, **maxit**, ϵ_{rel} , ϵ_{abs} , $\rho \in (0, 1]$, $k = 0$

1: **repeat**

2: Increment $k \leftarrow k + 1$

3: **Dirichlet step in Ω_1 :** solve

$$\begin{cases} \mathcal{R}_1(\mathbf{u}_1^{(k)}, \mathbf{v}) = 0 & \forall \mathbf{v} \in \mathcal{X}_{1,0} & \text{in } \Omega_1 \\ \gamma_1(\mathbf{u}_1^{(k)}) = \Pi_{12}\mathbf{g}^{(k)} & & \text{on } \Gamma_{12} \end{cases}$$

4: **Neumann step in Ω_2 :** solve

$$\begin{cases} \mathcal{R}_2(\mathbf{u}_2^{(k)}, \mathbf{v}) = 0 & \forall \mathbf{v} \in \mathcal{X}_{2,0} & \text{in } \Omega_2 \\ \Psi_2(\mathbf{u}_2^{(k)}) = -\Pi_{21}\Psi_1(\mathbf{u}_1^{(k)}) & & \text{on } \Gamma_{21} \end{cases}$$

5: **Classical relaxation:** Update $\mathbf{g}^{(k+1)} = (1 - \rho)\mathbf{g}^{(k)} + \rho\gamma_2(\mathbf{u}_2^{(k)})$

6: **until** $e_{\text{abs}}^{(k)} > \epsilon_{\text{abs}}$ **and** $e_{\text{rel}}^{(k)} > \epsilon_{\text{rel}}$ **and** $k < \text{maxit}$

7: **Output:** $\mathbf{u}_1^{(k)}$, $\mathbf{u}_2^{(k)}$

The interaction between sub-domains is encoded in the compatibility constraint on the continuity of the solution on interface Γ_{12} , and on the continuity of normal fluxes on Γ_{21} . Since the Dirichlet–Neumann iteration procedure gives an infinite sequence, it is necessary to define convergence criteria for the algorithm. The convergence criteria employed herein are given in Algorithm 1, line 6. Here, ϵ_{abs} and ϵ_{rel} are pre-specified absolute and relative tolerances,

respectively, and

$$\begin{aligned}
e_{\text{abs}}^{(k)} &:= \sqrt{\left\| \gamma_1(\mathbf{u}_1^{(k)}) - \gamma_1(\mathbf{u}_1^{(k-1)}) \right\|_2^2 + \left\| \gamma_2(\mathbf{u}_2^{(k)}) - \gamma_2(\mathbf{u}_2^{(k-1)}) \right\|_2^2}, \\
e_{\text{rel}}^{(k)} &:= \sqrt{\left\| \gamma_1(\mathbf{u}_1^{(k)}) - \gamma_1(\mathbf{u}_1^{(k-1)}) \right\|_2^2 / \left\| \gamma_1(\mathbf{u}_1^{(k)}) \right\|_2^2 + \left\| \gamma_2(\mathbf{u}_2^{(k)}) - \gamma_2(\mathbf{u}_2^{(k-1)}) \right\|_2^2 / \left\| \gamma_2(\mathbf{u}_2^{(k)}) \right\|_2^2}.
\end{aligned} \tag{4}$$

We choose to adopt stopping criteria based solely on interface quantities, as the Dirichlet–Neumann iteration is governed by the satisfaction of compatibility conditions on Γ_{12} and Γ_{21} . We note that alternative convergence criteria based on full sub-domain solution norms, such as those in [3, 4], are also possible; however, it can be shown that control of the error/traces on the interfaces implies control of the error in the full subdomains, hence interface-based stopping criteria are equivalent to sub-domain-based ones up to constants depending on the problem and norms used [30, 31]. In all of our numerical experiments, the proposed interface-based criteria were sufficient to reliably detect convergence.

At this point, it is worthwhile to point the reader’s attention to line 5 in Algorithm 1, which introduces a common Schwarz acceleration technique referred to herein as “classical relaxation”. It has been shown in several references, e.g., [15, 16], that adding relaxation of this form to the Dirichlet step of the Schwarz iteration procedure can speed up, and, in some cases, enable, convergence. The value $\rho \in (0, 1]$ in Algorithm 1, line 5, known as the “relaxation parameter”, is a constant pre-specified value, and one of the tuning knobs in the algorithm. The scheme in Algorithm 1 has been shown to converge in the case of coercive elliptic problems, as well as for problems described by skew-symmetric bilinear forms where the skew-symmetric part is small enough, c.f., [32, 33].

Remark 2. The approach described in Algorithm 1 solves the Dirichlet and Neumann problems (lines 3 and 4, respectively) sequentially; that is, the Ω_2 solve at iteration k cannot proceed until $\mathbf{u}_1^{(k)}$ has been calculated. This procedure is commonly referred to in the literature as “multiplicative Schwarz”. An alternative option, referred to as “additive Schwarz”, relies on the previously computed solution $\mathbf{u}_1^{(k-1)}$ when solving the Neumann problem in line 4 of Algorithm 1, making the algorithm embarrassingly parallel. It can be shown that the multiplicative and additive Schwarz variants converge to the same solution, though the latter method often requires more iterations to reach convergence [31, 34]. Herein, we focus on the multiplicative Schwarz

scheme, as it is possible to formulate various relaxed and accelerated versions of this method as a fixed-point iteration (see Section 2.3 and Remark 3), which enables certain theoretical analyses (Section 2.4).

2.3. Reformulation of multiplicative Schwarz as a fixed-point iteration method

The Dirichlet and Neumann BCs in Algorithm 1 can be seen as the outputs of suitable Dirichlet-to-Neumann (DtN) and Neumann-to-Dirichlet (NtD) maps, which we define as $\Lambda : \mathcal{U}_1 \rightarrow \mathcal{U}_1^*$, $\Upsilon : \mathcal{U}_2^* \rightarrow \mathcal{U}_2$ respectively, where

$$\Lambda : \Pi_{12}\gamma_2(\mathbf{u}_2) \mapsto \Psi_1(\mathbf{u}_1), \quad (5a)$$

$$\Upsilon : -\Pi_{21}\Psi_1(\mathbf{u}_1) \mapsto \gamma_2(\mathbf{u}_2). \quad (5b)$$

The DtN and NtD operators are understood as solution operators corresponding to their respective sub-domain problems. After introducing these maps, we can rewrite

$$\gamma_2(\mathbf{u}_2^{(k)}) = \Upsilon(-\Pi_{21}\Psi_1(\mathbf{u}_1^{(k)})) = \Upsilon(-\Pi_{21}(\Lambda(\Pi_{12}\mathbf{g}^{(k)}))),$$

so that, from the relaxation formula in line 5 of Algorithm 1, we obtain

$$\mathbf{g}^{(k+1)} = (1 - \rho)\mathbf{g}^{(k)} + \rho\Upsilon\left(-\Pi_{21}(\Lambda(\Pi_{12}\mathbf{g}^{(k)}))\right), \quad (5c)$$

a fixed-point equation on \mathbf{g} . Now, we define the operator $T : \mathcal{U}_2 \rightarrow \mathcal{U}_2$ such that

$$T(\mathbf{g}) = \Upsilon\left(-\Pi_{21}(\Lambda(\Pi_{12}\mathbf{g}))\right). \quad (5d)$$

Importantly, equation (5c) can be rewritten as

$$\mathbf{g}^{(k+1)} = T_\rho^r(\mathbf{g}^{(k)}) \quad (5e)$$

for a suitable operator $T_\rho^r : \mathcal{U}_2 \rightarrow \mathcal{U}_2$. This generalizes the standard method into a classical one-step fixed-point iteration for any suitable choice of ρ .

Thanks to the reformulation in (5c), we can restate Algorithm 1 in a more concise form of a fixed-point iteration algorithm, as done in Algorithm 2. As observed in [35], the formulation in (5c) does not involve the values of the solutions inside the sub-domains Ω_i , as all the operators are defined on the interface Γ . Hence, it is possible to apply the Schwarz alternating method using only interface data, and recover the full sub-domain solutions \mathbf{u}_1 and \mathbf{u}_2 at the end of the iteration procedure (Algorithm 2). The absolute and relative errors appearing in line 6 of Algorithm 2 can be computed using formula (4) with $\gamma_1(\mathbf{u}_1^{(k)}) = \Pi_{12}\mathbf{g}^{(k)}$ and $\gamma_2(\mathbf{u}_2^{(k)}) = T(\mathbf{g}^{(k)})$.

Algorithm 2 Dirichlet-Neumann scheme (with relaxation) as a fixed-point iteration.

Require: Initial guess $\mathbf{g}^{(1)}$, **maxit**, ϵ_{rel} , ϵ_{abs} , ρ , $k = 0$

1: **repeat**

2: Increment $k \leftarrow k + 1$

3: Update $\mathbf{g}^{(k+1)} = (1 - \rho)\mathbf{g}^{(k)} + \rho T(\mathbf{g}^{(k)})$

4: **until** $e_{\text{abs}}^{(k)} > \epsilon_{\text{abs}}$ **and** $e_{\text{rel}}^{(k)} > \epsilon_{\text{rel}}$ **and** $k < \text{maxit}$

5: **Output:** $\mathbf{u}_1^{(k)}$, $\mathbf{u}_2^{(k)}$

Remark 3. In the case of the additive variant of the Schwarz alternating method (see Remark 2), achieving the one-step fixed-point iteration (5e) is more nuanced. Because the local sub-problems are solved simultaneously, the transmission conditions evaluated on Γ_{ij} depend on the solutions from the previous iteration step, in particular the Neumann transmission condition would be dependent on $\Psi_1(\mathbf{u}^{(k-1)})$ on Γ_{21} . Thus, we would obtain, in place of (5c), a two-step iterative scheme of the form

$$\mathbf{g}^{(k+1)} = (1 - \rho)\mathbf{g}^{(k)} + \rho T(\mathbf{g}^{(k-1)}). \quad (6)$$

Although (6) is not a fixed-point iteration in the classical sense, it can be rigorously recast as a generalized one-step fixed-point iteration by augmenting the state space into $\bar{\mathbf{g}} = [\mathbf{g}^{(k)}, \mathbf{g}^{(k-1)}]^T$. The additive iteration can then be written as $\bar{\mathbf{g}}^{(k+1)} = \bar{T}(\bar{\mathbf{g}}^{(k)})$, where the augmented operator \bar{T} is defined as

$$\bar{T}(\mathbf{v}_1, \mathbf{v}_2) := ((1 - \rho)\mathbf{v}_1 + \rho T(\mathbf{v}_2), \mathbf{v}_1). \quad (7)$$

It is straightforward to verify that any fixed-point $[\mathbf{v}_1^*, \mathbf{v}_2^*]^T$ of this extended operator \bar{T} necessarily satisfies $\mathbf{v}_1^* = \mathbf{v}_2^*$, which immediately implies $\mathbf{v}_1^* = T(\mathbf{v}_1^*)$.

2.4. Schwarz acceleration techniques

2.4.1. Aitken acceleration

The classical relaxation introduced in Algorithm 1, line 5 assumes that ρ is a fixed pre-specified parameter. The “optimal” value of ρ is generally unknown *a priori*, and poor choices of this parameter can lead to convergence issues, as discussed in [23] and [7]. As demonstrated in [27] for the specific case of a two sub-domain fluid-structure interaction problem, it is possible to derive a relaxation scheme in which ρ is updated dynamically throughout

the Schwarz iteration process by applying Aitken acceleration to the fixed-point version of the Schwarz alternating method (Algorithm 2). The scheme is defined by first introducing the interface jump $\mathcal{E} : \mathcal{U}_2 \times \mathcal{U}_2 \rightarrow \mathbb{R}^{N^c d}$ (where N^c is the number of interface nodes of Γ_{21})

$$\mathcal{E} \left(\gamma_1^1(\mathbf{u}_1), \gamma_2(\mathbf{u}_2) \right) = \gamma_2(\mathbf{u}_2) - \gamma_1^2(\mathbf{u}_1), \quad (8)$$

together with the following variables:

$$\mathbf{d}^{(k)} = \left(\gamma_1^2(\mathbf{u}_1^{(k)}) - \gamma_1^2(\mathbf{u}_1^{(k-1)}) \right), \quad \boldsymbol{\delta}^{(k)} = \mathcal{E} \left(\gamma_1^1(\mathbf{u}_1^{(k)}), \gamma_2(\mathbf{u}_2^{(k)}) \right) - \mathcal{E} \left(\gamma_1^1(\mathbf{u}_1^{(k-1)}), \gamma_2(\mathbf{u}_2^{(k-1)}) \right).$$

Now, to apply Aitken acceleration within the Dirichlet-Neumann Schwarz scheme, line 5 in Algorithm 1 is replaced by

$$\mathbf{g}^{(k+1)} = \mathbf{g}^{(k)} + \rho^{(k)} \mathcal{E} \left(\gamma_1^1(\mathbf{u}_1^{(k)}), \gamma_2(\mathbf{u}_2^{(k)}) \right), \quad \text{where } \rho^{(k)} = -\frac{\boldsymbol{\delta}^{(k)} \cdot \mathbf{d}^{(k)}}{\|\boldsymbol{\delta}^{(k)}\|_2^2} \quad (9)$$

Here, $\rho^{(k)}$ denotes the value of the relaxation parameter at the k^{th} Schwarz iteration, with $\rho^{(1)}$ given as an input. The value of $\rho^{(k)}$ in (9) minimizes

$$\mathcal{J}(\rho) = \left\| \left(\gamma_1^2(\mathbf{u}_1^{(k)}) - \gamma_1^2(\mathbf{u}_1^{(k-1)}) \right) + \rho \left(\gamma_2(\mathbf{u}_2^{(k)}) - \gamma_1^2(\mathbf{u}_1^{(k)}) - \gamma_2(\mathbf{u}_2^{(k-1)}) + \gamma_1^2(\mathbf{u}_1^{(k-1)}) \right) \right\|_2^2. \quad (10)$$

at each Schwarz iteration $k = 1, \dots, \text{maxit}$ (see Appendix A).

Our Aitken-accelerated Schwarz scheme is summarized in Algorithm 3. The reader can observe that we have introduced a parameter $N_0 \in \mathbb{N}$ such that, for $1 < k < N_0$, $\rho^{(k)} = \rho^{(1)}$. As far as we know, the introduction of N_0 into the Aitken acceleration approach has not been considered in past literature.

Remark 4. It is possible to rewrite the Aitken formula (9) using the previously-defined DtN and NtD maps, as done for the classical relaxation formula in (5c):

$$\mathbf{g}^{(k+1)} = \mathbf{g}^{(k)} + \rho^{(k)} \left[T(\mathbf{g}^{(k)}) - \mathbf{g}^{(k)} \right] \quad \text{with } \rho^{(k)} = \rho^{(k)}(\mathbf{g}^{(k)}, \mathbf{g}^{(k-1)}). \quad (11)$$

In (11), we have explicitly expressed the dependence of the parameter $\rho^{(k)}$ on the current and previous interface solutions. Unlike (5c), the iteration in (11) is not a single fixed-point equation in the classical sense, as the dynamic parameter $\rho^{(k)}$ is a function of the interface data at iteration $k-1$. A similar discussion to Remark 3 can be replicated in this case.

Algorithm 3 Dirichlet-Neumann scheme with Aitken acceleration

Require: Initial guess $\mathbf{g}^{(1)}$, maxit , ϵ_{rel} , ϵ_{abs} , $\rho^{(1)}$, $k = 0$, N_0

```
1: repeat
2:   Increment  $k \leftarrow k + 1$ 
3:   if  $k < N_0$  then
4:      $\rho^{(k)} = \rho^{(1)}$ 
5:   else
6:      $\rho^{(k)}$  dynamically updated from (9)
7:   end if
8:   Update  $\mathbf{g}^{(k+1)} = (1 - \rho^{(k)})\mathbf{g}^{(k)} + \rho^{(k)} [T(\mathbf{g}^{(k)}) - \mathbf{g}^{(k)}]$ 
9: until  $e_{\text{abs}}^{(k)} > \epsilon_{\text{abs}}$  and  $e_{\text{rel}}^{(k)} > \epsilon_{\text{rel}}$  and  $k < \text{maxit}$ 
10: Output:  $\mathbf{u}_1^{(k)}$ ,  $\mathbf{u}_2^{(k)}$ 
```

Remark 5. The Aitken formula for $\rho^{(k)}$ (9) does not guarantee explicit upper or lower bounds for the relaxation parameter. To ensure consistency with the classical relaxation framework (Algorithm 1) and to avoid nonphysical values, we enforce in our numerical implementation of Aitken-accelerated Schwarz the following safeguards: (i) we set $\rho^{(k)} = 1$ whenever Aitken's formula (9) gives $\rho^{(k)} > 1$, and (ii) we revert to $\rho^{(k)} = \rho^{(1)}$ whenever a negative value is obtained.

2.4.2. Analysis of the Aitken-accelerated Schwarz scheme

Having presented the general Aitken-accelerated Schwarz scheme, we now perform some theoretical analysis to uncover its convergence rate for the specific case of $d = 1$. We recall that a p -order method converges to its fixed-point g^* if

$$\exists c > 0 : \frac{|g^{(k+1)} - g^*|}{|g^{(k)} - g^*|^p} \leq c, \forall k \geq k_0$$

where k_0 is a suitable integer and, in the case $p = 1$, we need to strictly require $0 < c < 1$.

Theorem 1. Suppose $d = 1$. Let $g^{(k+1)} = T(g^{(k)})$ be the fixed-point iteration of an unrelaxed Schwarz scheme (line 3 in Algorithm 2 with $\rho = 1$). Assuming that the unrelaxed Schwarz method converges linearly ($p = 1$), the Aitken-accelerated Schwarz algorithm (Algorithm 3) converges to g^* quadratically ($p = 2$).

Proof. Let $e_k = g^{(k)} - g^*$ denote the convergence error at iteration k . We have that $\lim_{k \rightarrow \infty} \frac{|e_{k+1}|}{|e_k|} = |\lambda|$ with the convergence factor $0 < |\lambda| < 1$ in order for $g^{(k)}$ to converge to g^* . Now, the error can be written as

$$e_{k+1} = \lambda e_k + O(|e_k|^2), \quad (12a)$$

assuming that the fixed-point operator T is sufficiently smooth (specifically, at least locally of class C^2 near g^*). In the scalar case, the quantities appearing in Aitken formula simplify to:

$$d^{(k)} = g^{(k)} - g^{(k-1)} = e_k - e_{k-1} = (\lambda - 1)e_{k-1} + O(|e_{k-1}|^2), \quad (12b)$$

$$\delta^{(k)} = \mathcal{E}^{(k)} - \mathcal{E}^{(k-1)} = ad^{(k)} = a(\lambda - 1)e_{k-1} + O(|e_{k-1}|^2), \quad (12c)$$

where we assume that the interface residual is linear in the interface unknown, i.e., $\mathcal{E}^{(k)} = ae_k$ with $a \in \mathbb{R}_0$. It follows that Aitken parameter $\rho^{(k)}$ reduces to

$$\rho^{(k)} = -\frac{1}{a} + O(|e_{k-1}|). \quad (12d)$$

From the interface update formula with Aitken acceleration (c.f., (9)), $g^{(k+1)} = g^{(k)} + \rho^{(k)}\mathcal{E}^{(k)}$. Now, using (12a) and (12b), we have that

$$e_{k+1} = e_k + \rho^{(k)}ae_k \quad (12e)$$

$$= \lambda e_{k-1} + O(|e_{k-1}|^2) + \rho^{(k)}[a\lambda e_{k-1} + O(|e_{k-1}|^2)] \quad (12f)$$

$$= O(|e_{k-1}|^2), \quad (12g)$$

where the last equality is derived by replacing in it the expression on $\rho^{(k)}$ in (12d). We have thus demonstrated that the linear term in the error drops out, so that the Aitken error scales only with the quadratic term $|e_{k-1}|^2$. The Aitken convergence rate is thus equal to two, since

$$\frac{|e_{k+1}|}{|e_k|^2} \leq C \frac{|e_{k-1}|^2}{|e_k|^2} = C \left(\frac{e_{k-1}}{e_k} \right)^2 \leq C \left(\frac{1}{|\lambda| - \epsilon} \right)^2 < \infty$$

where $\epsilon = \mathcal{O}(|e_{k-1}|^2)$. The first inequality for $C > 0$ is derived from the result in (12g) and, in the last inequality, we used the assumption that unrelaxed Schwarz has a linear convergence rate, i.e.

$$\begin{aligned} \frac{|e_k|}{|e_{k-1}|} = |\lambda| + O(|e_{k-1}|^2), & \implies \text{for } k \text{ large enough, } \exists \epsilon > 0: \quad |\lambda| - \epsilon \leq \frac{|e_k|}{|e_{k-1}|} \leq |\lambda| + \epsilon \\ & \implies \frac{1}{|\lambda| + \epsilon} \leq \frac{|e_{k-1}|}{|e_k|} \leq \frac{1}{|\lambda| - \epsilon}. \end{aligned}$$

□

Remark 6. Convergence of the Aitken-accelerated sequence actually just requires the *local* linear convergence of the base fixed-point iteration, i.e., in the proof of Theorem 1, we actually just needed $0 < |\lambda| < 1$ in a neighborhood of g^* . Indeed, once the fixed-point iterates enter the linear regime near g^* , Aitken acceleration guarantees quadratic convergence to g^* , irrespective of any weaker global convergence properties of the fixed-point map.

Remark 7. When $d > 1$, there is no general result guaranteeing quadratic convergence of the Aitken-accelerated vector sequence without additional structure (a dominant eigenvector or a 1D invariant subspace). The acceleration can at best damp or cancel the dominant 1D component, but the full vector error may not be reduced quadratically in general. As we describe in Section 3 for a two-dimensional (2D) study case, a super-linear/quadratic convergence can be achieved by Aitken-accelerated Schwarz for some values of N_{dd} .

2.4.3. Anderson acceleration

An alternate method that has been shown to speed up the convergence of fixed-point iterations is Anderson acceleration [24]. Here, we adapt this approach to the specific case of the non-overlapping Schwarz alternating method, which can be written as a fixed-point iteration, as shown above. To the best of our knowledge, our theoretical and numerical assessment of Anderson-accelerated non-overlapping Schwarz is one of the novel contributions of this work.

The basic non-overlapping Schwarz Dirichlet-Neumann scheme with Anderson acceleration is given in Algorithm 4. The reader can observe that a new algorithmic parameter is introduced, $m_{\text{and}} \in \mathbb{N}_0$, which represents the maximum history of the previous steps that we want to include in the update of $\mathbf{g}^{(k)}$. The basic version of the algorithm sets $m_k = \min(k, m_{\text{and}})$ (Algorithm 4, line 4). We introduce in line 5 of Algorithm 4 the history residual matrix $\mathbf{F}_k \in \mathbb{N}^{N^c d \times (m_k + 1)}$, which stores in its columns the last $m_k + 1$ fixed-point residuals $\mathbf{f}_i = T(\mathbf{g}^{(i)}) - \mathbf{g}^{(i)}$ with $i = k - m_k, \dots, k$, and defines the history for Schwarz iteration k . The Dirichlet and Neumann problems in lines 3 and 4 of the classical Schwarz algorithm, Algorithm 1, are encoded in step 5 of Algorithm 4 in the evaluation of the operator $T(\mathbf{g})$. The reader can observe that Algorithm 4 includes a pre-specified relaxation parameter $\rho \in (0, 1]$, similar to the classical relaxed Dirichlet-Neumann scheme (Algorithm 1). Some analysis of relaxed Anderson acceleration can be found in [36]. While it is common to simplify the Anderson acceleration scheme

by setting $\rho = 1$, herein we choose to explore the impact of this parameter on Schwarz convergence and robustness (see Section 3). Our results suggest that Anderson-accelerated Schwarz is far less sensitive to ρ than Schwarz with classical relaxation, often exhibiting convergence even in the unrelaxed ($\rho = 1$) case.

Algorithm 4 Dirichlet–Neumann scheme with Anderson acceleration (and no memory adaptation) as a fixed-point iteration.

Require: Initial guess $\mathbf{g}^{(0)}$, maxit , ϵ_{rel} , ϵ_{abs} , $k = 0$, m_{and} , ρ

1: Compute $\mathbf{g}^{(1)} = T(\mathbf{g}^{(0)})$

2: **repeat**

3: Increment $k \leftarrow k + 1$

4: Define $m_k = \min(k, m_{\text{and}})$

5: Set the residual matrix $\mathbf{F}_k = [\mathbf{f}_{k-m_k}, \dots, \mathbf{f}_k]$ where $\mathbf{f}_i = T(\mathbf{g}^{(i)}) - \mathbf{g}^{(i)}$.

6: Determine $\boldsymbol{\alpha}^{(k)} = [\alpha_0^{(k)}, \dots, \alpha_{m_k}^{(k)}]^T$ that solve

$$\min_{\boldsymbol{\alpha}=[\alpha_0, \dots, \alpha_{m_k}]^T} \|\mathbf{F}_k \boldsymbol{\alpha}\|_2 \quad \text{s.t.} \quad \sum_{i=0}^{m_k} \alpha_i = 1 \quad (13)$$

7: Set

$$\mathbf{g}^{(k+1)} = (1 - \rho) \sum_{j=0}^{m_k} \alpha_j^{(k)} \mathbf{g}^{(k-m_k+j)} + \rho \sum_{j=0}^{m_k} \alpha_j^{(k)} T(\mathbf{g}^{(k-m_k+j)}) \quad (14)$$

8: **until** $e_{\text{abs}}^{(k)} > \epsilon_{\text{abs}}$ **and** $e_{\text{rel}}^{(k)} > \epsilon_{\text{rel}}$ **and** $k < \text{maxit}$

9: **Output:** $\mathbf{u}_1^{(k)}, \mathbf{u}_2^{(k)}$

2.4.4. Comparisons to and connections with Aitken acceleration

Having introduced the Anderson-accelerated Schwarz scheme, we now make some comparisons and connections between this scheme and Aitken-accelerated Schwarz.

First, when $m_{\text{and}} = 1$ and $\rho = 1$ (no relaxation), equation (14) takes the form

$$\mathbf{g}^{(k+1)} = \alpha_0^{(k)} T(\mathbf{g}^{(k-1)}) + \alpha_1^{(k)} T(\mathbf{g}^{(k)}), \quad (15)$$

which represents an update based on the two previous iterations, as in Aitken acceleration. For $m_{\text{and}} > 1$, the formula in (15) is enriched with $m_k + 1$ terms of the form $g^{(k-(m_k+1))}, \dots, g^{(k)}$.

Returning to the more general case of Anderson acceleration with $m_{\text{and}} > 1$, we show that Anderson and Aitken acceleration can be interpreted as multi-secant and single-secant quasi-Newton methods, respectively. These interpretations have implications for the expected convergence of the Schwarz alternating method accelerated with these schemes.

As shown in [24], the original constrained Anderson least-squares problem (13) can be recast as an unconstrained residual minimization involving residual differences. Using the constraint in (13), the last Anderson coefficient takes the form $\alpha_{m_k} = 1 - \sum_{i=0}^{m_k-1} \alpha_i$. Substituting this value into the objective function in (13) gives rise to the following equivalent form

$$\min_{\gamma=[\gamma_0, \dots, \gamma_{m_k-1}]^T} \|\mathbf{f}_k - \mathcal{F}^{(k)}\gamma\|_2^2, \quad (16)$$

for coefficients vector $\gamma \in \mathbb{R}^{m_k}$ with $\mathcal{F}^{(k)} = (\Delta\mathbf{f}_{k-m_k}, \dots, \Delta\mathbf{f}_{k-1})$ and $\Delta\mathbf{f}_k := \mathbf{f}_k - \mathbf{f}_{k-1}$. If we define $\mathbf{U}^{(k)} = (\Delta\mathbf{g}^{(k-m_k)}, \dots, \Delta\mathbf{g}^{(k-1)})$ with $\Delta\mathbf{g}^{(k)} = \mathbf{g}^{(k+1)} - \mathbf{g}^{(k)}$, the minimization problem (16) can be interpreted as a multi-secant quasi-Newton method with associated multi-secant equation

$$\mathbf{U}^{(k)} = \mathbf{G}^{(k)}\mathcal{F}^{(k)}. \quad (17)$$

Here, $\mathbf{G}^{(k)}$ is an approximation of the inverse of the Jacobian of $\mathbf{f}_k = T(\mathbf{g}^{(k)}) - \mathbf{g}^{(k)}$. In contrast, it is straightforward to see that Aitken acceleration is associated with a single-secant quasi-Newton update. As shown in Section 2.4.1, the Aitken acceleration parameter $\rho^{(k)}$ is obtained by minimizing the functional (10) involving only the most recent solution pair of solutions. This least-squares minimization problem corresponds to a secant equation of the general form $\Delta\mathbf{g}^{(k)} = \mathbf{G}^{(k)}\Delta\mathbf{f}_k$, which is written explicitly in (9). The reader can observe from this equation that the inverse Jacobian $\mathbf{G}^{(k)}$ is being approximated by a scalar multiple of the identity. It is well-known that a multi-secant method approximates the Jacobian inverse more accurately than the single secant technique; hence, Anderson-accelerated Schwarz is expected to be more robust, especially when applied to large-scale multi-dimensional problems decomposed into large numbers of subdomains. This claim is explored numerically in Section 3.

Finally, we compare Aitken- and Anderson-accelerated Schwarz from the perspective of implementation and usability. It is clear that, for $m_{\text{and}} > 1$,

Anderson-accelerated Schwarz has a larger memory footprint and gives rise to a more involved implementation. While we would expect for Anderson-accelerated Schwarz to have a larger CPU time per iteration due to the need to solve the minimization problem (13) at each Schwarz iteration k , our numerical results demonstrate that this is actually not the case in practice, at least in our implementation (see Section 3).

2.4.5. Analysis of the Anderson-accelerated Schwarz scheme

In the following theorem, we analyze the Anderson optimization coefficients α_j in terms of the spectral properties of the fixed-point operator T for the specific case of $d = 1$.

Theorem 2. The Anderson coefficients $\alpha \in \mathbb{R}^{m_k+1}$ obtained by solving the constrained minimization problem (13) in the scalar limit follow a geometric distribution. Specifically, they take the form

$$\alpha_j = \frac{|\ell_{\max}|^j}{\sum_{i=0}^{m_k} |\ell_{\max}|^i} \text{ for } j = 0, \dots, m_k, \quad (18)$$

where $|\ell_{\max}| = \max\{|\lambda| : \lambda \in \sigma(T)\}$, with $\sigma(T)$ denoting the spectrum of the fixed-point operator T , assumed to be linear. If $|\ell_{\max}| = 1$, the coefficients reduce to the uniform weights $\alpha_j = \frac{1}{m_k+1}$.

Proof. Consider the fixed-point residuals $f_i = T(g^{(i)}) - g^{(i)} = T(g^{(i)}) - g^* + g^* - g^{(i)} = T(e_i) - e_i$. It follows that $f_k = T(e_k) - e_k$ and $f_{k+1} = T(e_{k+1}) - e_{k+1}$. By the hypothesis of asymptotic regime, we have that $T(e_{k+1}) \approx \ell_{\max} T(e_k)$. Indeed, since $g^{(k+1)} = T(g^{(k)})$ we have that $g^{(k+1)} - g^* = T(g^{(k)}) - g^*$, which implies $e_{k+1} = T(g^{(k)} - g^*) = T(e_k)$ since T is linear. As for the residuals, $f_{k+1} \approx \ell_{\max} T(e_k) - \ell_{\max} e_k = \ell_{\max} f_k$; thus $f_{k+1} \approx \ell_{\max} f_k$.

Using the last $m_k + 1$ Anderson history residuals f_{m-m_k}, \dots, f_k , we can write

$$|f_{k-j}| \approx |\ell_{\max}|^{-j} |f_k| \text{ for } j = 0, \dots, m_k \quad (19a)$$

Substituting these approximations into the Anderson objective function at iteration k (13), where $F_k \approx [\ell_{\max}^{-m_k} f_k, \dots, \ell_{\max}^{-1} f_k]$, we can recast (13) as a minimization problem for the weighted sum of squares

$$\min_{\alpha \in \mathbb{R}^{m_k}} \mathcal{J}_{\text{and}}(\alpha) = \sum_{j=0}^{m_k} \frac{1}{|\ell_{\max}|^j} \alpha_j^2 \text{ s.t. } \sum_{j=0}^{m_k} \alpha_j = 1, \quad (19b)$$

Problem (19b) represents a weighted variance minimization problem over the historical contributions. The associated Lagrangian is $\mathcal{L}(\boldsymbol{\alpha}, \mu) = \sum_{j=0}^{m_k} |\ell_{\max}|^{-j} \alpha_j^2 - \mu \left(\sum_{j=0}^{m_k} \alpha_j - 1 \right)$. The optimality conditions give

$$\alpha_j = \frac{\mu}{2} |\ell_{\max}|^j \quad \text{for each } j = 0, \dots, m_k. \quad (19c)$$

Substituting (19c) into the sum-to-one constraint yields $\frac{\mu}{2} = \frac{1}{\sum_{i=0}^{m_k} |\ell_{\max}|^i}$. By substituting this expression for $\mu/2$ into (19c), one obtains the result $\alpha_j = \frac{|\ell_{\max}|^j}{\sum_{i=0}^{m_k} |\ell_{\max}|^i}$. Finally, we observe that, if $|\ell_{\max}| = 1$, then (19b) is satisfied by the uniform weights solutions α_j s.t. $\alpha_j = \frac{1^j}{\sum_{i=0}^{m_k} 1^i} = \frac{1}{m_k+1}$. \square

Remark 8. While, in the general Anderson acceleration algorithm, the coefficients α_j can take negative values to orthogonalize the residuals, our derivation shows that, under the assumption of scalar case and dominant-eigenvalue decay, the coefficients asymptotically approach a positive geometric distribution.

2.4.6. Anderson with memory adaptation

As remarked in [24], if m_{and} is small, the secant information used by the method may be too limited to provide decidedly fast convergence, whereas if m_{and} is too large, the least-squares optimization problem for the $\boldsymbol{\alpha}$ coefficients (13) may be poorly conditioned. The most appropriate choice of m_{and} (and thus of m_k) is often problem- and DD-dependent, as we will show in Section 3.2.4. To mitigate this difficulty, we propose an adaptive variant of the method, which we term ‘‘Anderson with memory adaptation’’. In this version of the algorithm, the value of m_k is adapted on-the-fly using the following formula:

$$m_k := \begin{cases} \min(\bar{m}, m_{\text{and}}), & \text{for } |e_{\text{rel}}^{(k)} - e_{\text{rel}}^{(k-1)}| < \epsilon_{\text{and}} \text{ and } k > 2, \\ \min(k, m_{\text{and}}), & \text{otherwise.} \end{cases} \quad (20)$$

The criterion in (20) is based on the relative interface error at the current and previous Schwarz iterations and a prescribed threshold ϵ_{and} . The pre-selected parameter \bar{m} can be chosen as a small integer, since, for small interface errors, the loss of relevant information is negligible. In addition, a small \bar{m} discards outdated secant information from earlier iterations and keeps the constrained problem small. While the idea of adapting m_k on-the-fly is

mentioned in [24] (where the authors discuss the idea of dropping columns based on the condition number of the constrained minimization problem), the specific formula (20) for how to do this is new, to the best of our knowledge.

3. Numerical results

3.1. One-dimensional Laplace equation

We consider here a simple study case based on the 1D Laplace equation, with the goal of comparing the proposed relaxation and acceleration techniques for the non-overlapping Schwarz alternating method both numerically and theoretically. Letting $\Omega = (0, 1) \in \mathbb{R}$, the boundary value problem of interest is

$$\begin{cases} -u''(x) = 0 & \text{in } (0, 1) \\ u(0) = 0, \quad u(1) = 1. \end{cases} \quad (21a)$$

It is possible to derive analytically the exact solution to (21a): $u(x) = x$.

In applying the non-overlapping Schwarz alternating method, we will partition Ω into two sub-domains, with $\bar{x} \in (0, 1)$ denoting the interface point. As in the previous section, we denote by $g^{(k)}$ the interface data for the Dirichlet-Neumann Schwarz algorithm at iteration $k > 0$. The sub-solutions $u_1^{(k)}$ and $u_2^{(k)}$ are obtained by solving the following Dirichlet and Neumann problems in $\Omega_1 = (0, \bar{x})$ and $\Omega_2 = (\bar{x}, 1)$:

$$\begin{cases} -u_1^{(k)''}(x) = 0 & \text{in } (0, \bar{x}) \\ u_1^{(k)}(0) = 0 \\ u_1^{(k)}(\bar{x}) = g^{(k)} \end{cases}, \quad \begin{cases} -u_2^{(k)''}(x) = 0 & \text{in } (\bar{x}, 1) \\ u_2^{(k)}(1) = 1 \\ u_2^{(k)' }(\bar{x}) = u_1^{(k)' }(\bar{x}) \end{cases} \quad \text{and} \quad g^{(k+1)} = \gamma(u_2^{(k)}). \quad (21b)$$

In our numerical study, we apply the Dirichlet-Neumann Schwarz iteration procedure (21b) with classical relaxation, as well as with Aitken and Anderson acceleration. We discretize the problem in both Ω_1 and Ω_2 using a finite difference discretization with 20 uniformly-spaced points. As will become apparent later, the interface location \bar{x} is varied in our analyses. Errors are computed with respect to a reference solution in $\Omega := \Omega_1 \cup \Omega_2$, and the following algorithmic parameters are utilized: $g^{(1)} = 0.3$, $\text{maxiter} = 50$ and $\epsilon_{\text{abs}} = \epsilon_{\text{rel}} = 10^{-8}$.

Before presenting our numerical results, we introduce and prove the following theorem, which is referred to later on, when our results are analyzed.

Theorem 3. For the simple Laplace equation study case (21a) solved using the Aitken-accelerated Dirichlet-Neumann Schwarz scheme (21b) applied to two sub-domains with an interface at $x = \bar{x}$, the optimal Aitken parameter $\rho^{(k)}$ satisfies

$$\rho^{(k)} = \bar{x}. \quad (21c)$$

Proof. It is straightforward to show that

$$\gamma(u_2^{(k)}) = 1 - \frac{g^{(k)}}{\bar{x}}(1 - \bar{x}), \quad (21d)$$

so that the interface residual jump is $\mathcal{E}(\gamma(u_1), \gamma(u_2)) = \gamma(u_2) - g^{(k)} = 1 - \frac{g^{(k)}}{\bar{x}}$. Recall the Aitken formula for $\rho^{(k)}$ (9), which simplifies in the 1D setting to $\rho^{(k)} = -\frac{\delta^{(k)}d^{(k)}}{|\delta^{(k)}|^2}$ with $\delta^{(k)} = \mathcal{E}^{(k)} - \mathcal{E}^{(k-1)} = 1 - \frac{g^{(k)}}{\bar{x}} - [\gamma(u_2^{(k-1)}) - \gamma(u_1^{(k-1)})] = \frac{g^{(k-1)} - g^{(k)}}{\bar{x}}$ and $d^{(k)} = \gamma(u_1^{(k)}) - \gamma(u_1^{(k-1)}) = g^{(k)} - g^{(k-1)}$. It follows that, for the study case of interest, the optimal Aitken parameter is given by (21c). This result is consistent with the previous related study in [16]. \square

\bar{x}	Classical relaxation ρ values						Aitken ($N_0 = 2$)	Anderson
	0.1	0.2	0.5	0.7	0.8	1	$\rho^{(1)} = 1$	$\rho = 1$
0.1	2	maxit	maxit	maxit	maxit	maxit	3	3
0.2	24	2	25	maxit	maxit	maxit	3	3
0.5	50	33	2	20	35	maxit	3	3
0.7	maxit	maxit	15	2	11	23	3	3
0.8	maxit	maxit	19	10	2	14	3	3

Table 1: 1D Laplace equation. Number of Schwarz iterations required to reach convergence tolerances $\epsilon_{\text{abs}} = \epsilon_{\text{rel}} = 10^{-8}$ for different values of ρ and \bar{x} when employing classical relaxation, Aitken acceleration and Anderson acceleration.

\bar{x}	Classical relaxation ρ values						Aitken ($N_0 = 2$)	Anderson Aitken ($N_0 = 2$)
	0.1	0.2	0.5	0.7	0.8	1	$\rho^{(1)} = 1$	$\rho = 1$
0.1	5.6×10^{-17}	4×10^{-1}	10^{29}	10^{38}	10^{41}	10^{47}	2.22×10^{-16}	3.5×10^{-13}
0.2	6.0×10^{-9}	2.8×10^{-17}	8.9×10^{-9}	10^{19}	10^{22}	10^{29}	2.22×10^{-16}	5.2×10^{-12}
0.5	7.1×10^{-7}	6.4×10^{-9}	0	7.7×10^{-9}	9.2×10^{-9}	4.0×10^{-1}	0	3.13×10^{-11}
0.7	3.0×10^{-5}	7.9×10^{-9}	6.9×10^{-9}	0	10^{-9}	4.6×10^{-9}	0	3.44×10^{-11}
0.8	9.0×10^{-5}	9.4×10^{-8}	6.7×10^{-9}	3.2×10^{-9}	0	9.3×10^{-9}	0	3.61×10^{-11}

Table 2: 1D Laplace equation. Error ϵ_{abs} obtained at the last Schwarz iteration for different values of ρ and \bar{x} when employing classical relaxation, Aitken acceleration and Anderson acceleration.

3.1.1. Schwarz with classical relaxation

First, we present results for the non-overlapping Schwarz alternating method applied to (21a) accelerated using classical relaxation (Algorithm 1). Columns 2–7 of Table 1 report the number of Schwarz iterations required to reach convergence for several different values of the ρ parameter. Similarly, columns 2–7 of Table 2 report the errors obtained at the last Schwarz iteration for different values of ρ . The reader can observe that the best convergence and minimal error is reached for the choice of $\rho = \bar{x}$ for all the values of $\bar{x} \in (0, 1)$ tested (see the squares marked in green in Tables 1 and 2). This is consistent with the result in Theorem 3. In this case, the method converges in two iterations, since the stopping criterion is based on the difference between successive iterates, $e_{\text{abs}}^{(k)}$. With the optimal relaxation parameter, the interface iteration yields the exact interface value after the first iteration, so that the true error is already zero, i.e. $e_1 = |g^{(1)} - g^*| = |g^{(1)} - \bar{x}|$, as expected from our theoretical analysis. Figure 2(a) shows the solutions for Schwarz iterations $k = 1, 2$ when applying the optimal value of ρ in the Schwarz algorithm with classical relaxation: the solution at iteration two coincides with the exact solution.

We now attempt to explain theoretically the non-convergence cases in Tables 1 and 2, marked with a pink color. If we go back to the classical relaxation formula

$$g^{(k+1)} = (1 - \rho)g^{(k)} + \rho\gamma(u_2^{(k)})$$

and replace the last term with the value obtained for the trace of the solution to the Neumann problem (21d), we obtain

$$g^{(k+1)} = \left[1 - \frac{\rho}{\bar{x}}\right]g^{(k)} + \rho. \quad (21e)$$

Now, we know from the exact solution of (21a) that $g^* = \bar{x}$, where g^* is the solution to our fixed-point iteration problem. The fixed-point iteration error at iteration k can thus be written as $e_k = |g^{(k)} - g^*| = |g^{(k)} - \bar{x}|$. By using (21e), the error at iteration $k + 1$ now takes the form

$$e_{k+1} = \left|1 - \frac{\rho}{\bar{x}}\right| e_k,$$

so that the fixed-point iteration error decays with rate

$$\lambda(\rho) = \frac{e_{k+1}}{e_k} = \left|1 - \frac{\rho}{\bar{x}}\right| \quad (21f)$$

For convergence, we would need the following constraint: $|\lambda(\rho)| < 1$. In order for this to hold for (21f), we must have that $0 < \rho < 2\bar{x} < 2$, since $\bar{x} \in (0, 1)$. We observe, however, that for \bar{x} very small, we have that $\frac{\bar{x}-\rho}{\bar{x}} \sim -\frac{\rho}{\bar{x}}$: in this case, the condition would be that $-\frac{\rho}{\bar{x}} < 1$, which implies that we must have $\rho < \bar{x}$ for convergence. This explains the divergence cases highlighted in pink in Tables 1–2, which correspond to α being very small and/or $\rho > \bar{x}$. The analysis above implies that an at least superlinear convergence is expected when $\lambda = 0$. This case corresponds to the condition that $\rho = \bar{x}$, which coincides with the optimal $\rho^{(k)}$ derived in Theorem 3.

Finally, we observe that, for the case of no relaxation (i.e., $\rho = 1$), which corresponds to the yellow-shaded columns in Tables 1 and 2, the condition that the convergence factor $|\lambda(\rho)| < 1$ would require that $|\frac{\bar{x}-1}{\bar{x}}| < 1$, which implies that $\bar{x} > \frac{1}{2}$, using the assumption that $\bar{x} \in (0, 1)$. This theoretical result is confirmed by our numerical experiments: for $\bar{x} < \frac{1}{2}$ (the first three yellow rows), we observe a much slower convergence and, in some cases, actual divergence of the Schwarz alternating method.

3.1.2. Schwarz with Aitken acceleration

Next, we solve problem (21a) using Aitken-accelerated Schwarz with $\rho^{(1)} = 1$. We find that, for the same tested values of \bar{x} , just three iterations are needed to reach convergence (see the second-to-last columns of Tables 1 and 2). In this case, the true error is zero after the second iteration, since, at $k = 1$, we do not apply Aitken yet. In Figure 2(b) the solutions at iteration $k = 1, 2, 3$ are depicted. Not only is the optimal value $\rho^* = \bar{x}$ obtained within the algorithm upon convergence, the Aitken acceleration algorithm detects this value for all k , as well as for all values of \bar{x} tested. This numerical result is consistent with the theoretical result in (21c).

3.1.3. Schwarz with Anderson acceleration

To complete this brief analysis, we lastly consider Anderson-accelerated Schwarz for the specific values of $m_{\text{and}} = 1$ and $\rho = 1$ (no relaxation) in the Anderson acceleration algorithm (c.f., (14)). Since $m_{\text{and}} = 1$, Anderson with memory adaptation (Section 2.4.6) is not relevant. The reader can observe from examining the last columns of Tables 1 and 2 that the Anderson-accelerated Schwarz converges in just three iterations to a solution whose error is close to machine precision.

We now demonstrate that this numerical result is expected theoretically. By computing the sub-solutions to (21b) in Ω_1 and Ω_2 we obtain

that $T(g^{(k)}) = \left(1 - \frac{1}{\bar{x}}\right) g^{(k)} + 1$. The Anderson update in the unrelaxed case takes the form (c.f., (14))

$$g_{\text{and}}^{(k+1)} = \alpha_0 T(g^{(k-1)}) + \alpha_1 T(g^{(k)}), \quad (21g)$$

where we explicitly indicated with the subscript and that the new datum g is found using the Anderson acceleration algorithm. The coefficients α_0 and α_1 solve the constrained minimization problem (c.f., (13))

$$\min_{\tilde{\alpha}_0, \tilde{\alpha}_1} |\tilde{\alpha}_0 f_{k-1} + \tilde{\alpha}_1 f_k| \quad \text{s.t.} \quad \tilde{\alpha}_0 + \tilde{\alpha}_1 = 1,$$

with $f_{k-1} = 1 - \frac{g^{(k-1)}}{\bar{x}}$ and $f_k = 1 - \frac{g^{(k)}}{\bar{x}}$. The reader can easily check that the solutions to the minimization problem are

$$\alpha_0 = \frac{g^{(k)} - \bar{x}}{g^{(k)} - g^{(k-1)}}, \quad \alpha_1 = \frac{\bar{x} - g^{(k-1)}}{g^{(k)} - g^{(k-1)}},$$

and thus we obtain the following update for the new iteration ($k = 2$):

$$g_{\text{mix}} := \alpha_0 g^{(k-1)} + \alpha_1 g^{(k)} = \bar{x} = g^*. \quad (21h)$$

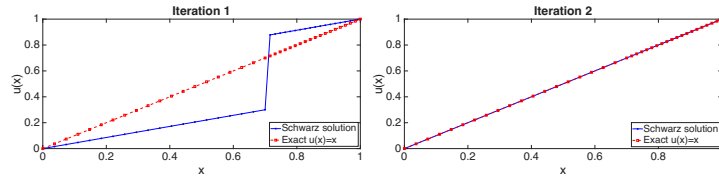
Since T is an affine map in this simple study case, we can write

$$g_{\text{and}}^{(k+1)} = \alpha_0 T(g^{(k-1)}) + \alpha_1 T(g^{(k)}) = T(\alpha_0 g^{(k-1)} + \alpha_1 g^{(k)}) = T(g_{\text{mix}}) = T(g^*) = g^*$$

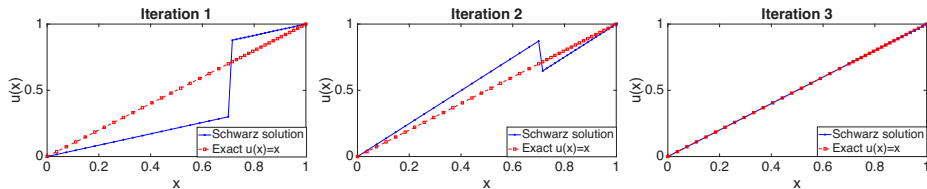
by using (21h) and the definition of the operator T .

The above analysis shows that, for this simple study case, the Anderson-accelerated Schwarz method (Algorithm 4) should produce the exact fixed-point solution in just one acceleration step, after the two history-steps required to compute $g^{(k-1)}$ and $g^{(k)}$. This result is numerically verified in the last columns of Tables 1 and 2.

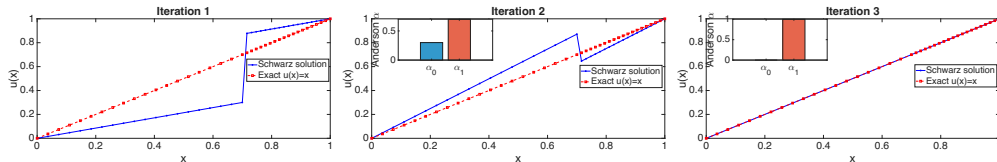
Finally, in Figure 2(c) the Anderson-accelerated Schwarz solution is depicted for different Schwarz iterations. Discarding iteration $k = 1$, for which the Anderson history matrix F_k is empty, we can numerically compute the solutions to the constrained minimization problem (13). The resulting optimal values of α_0 and α_1 are shown as histograms super-imposed on top of the solution plots in Figure 2(c). The reader can observe that the asymptotic value of $\boldsymbol{\alpha}^*$ is $[0, 1]^T$. Since the Anderson residual is 0 after the first two iterations which create the history required to apply the approach, the constrained problem (13) is solved by zeroing the old non-negligible residual (by setting $\alpha_0 = 0$) and choosing $\alpha_1 = 1$ to satisfy the constraint.



(a) Schwarz solutions with classical relaxation and the optimal choice of ρ for iteration $k = 1$ (left) and $k = 2$ (right)



(b) Aitken-accelerated Schwarz solutions for iterations $k = 1$ (left), $k = 2$ (middle) and $k = 3$ (right)



(c) Anderson-accelerated Schwarz solutions for iterations $k = 1$ (left), $k = 2$ (middle) and $k = 3$ (right)

Figure 2: 1D Laplace equation. (a) Classical relaxation-accelerated Schwarz solutions with the optimal choice of $\rho = \bar{x}$. (b) Aitken accelerated Schwarz solutions with $\rho^{(1)} = 1$. (c) Unrelaxed Anderson-accelerated Schwarz solutions. The middle and right sub-plots in (c) also show the values of α_0 and α_1 in histogram form for $k = 2$ and $k = 3$, respectively. All subplots are for the specific case of $\bar{x} = 0.7$.

3.2. Two-dimensional nonlinear elasticity

For our second example, we numerically study the convergence of the Dirichlet-Neumann Schwarz alternating method with different relaxation/acceleration strategies for a steady nonlinear elasticity problem. In particular, we compare the numerical performance of the relaxation and acceleration methods summarized in Section 2.4 on a 2D simplification of the cuboid test proposed in [3]. More specifically, we solve a nonlinear elasticity problem $-\nabla \cdot \mathbf{P}(\mathbf{F}(\mathbf{u})) = \mathbf{0}$ in Ω expressed in terms of the the deformation gradient $\mathbf{F}(\mathbf{u}) = \mathbb{I} + \nabla \mathbf{u}$ and the displacement \mathbf{u} . The stress tensor is given by the first Piola-Kirchhoff stress tensor \mathbf{P} :

$$\mathbf{P}(\mathbf{F}) = \lambda_2 (\mathbf{F} - \mathbf{F}^{-T}) + \lambda_1 (\log(\det(\mathbf{F}))) \mathbf{F}^{-T}, \quad (22)$$

implying a Neo-Hookean-type material model [37]. The Lamé constants λ_1 and λ_2 are defined in terms of the Young's modulus E and Poisson's ratio ν as $\lambda_1 = \frac{E\nu}{(1+\nu)(1-2\nu)}$, $\lambda_2 = \frac{E}{2(1+\nu)}$. We depict, in Figure 3(a), the global computational domain together with the system boundaries, denoted by Σ_i for $i = 1, \dots, 4$. The problem is characterized by the following Dirichlet BCs: $\mathbf{u} \cdot \mathbf{n} = 0$ at boundaries Σ_1 and Σ_3 ; $\mathbf{u} \cdot \mathbf{n} = 1$ on boundary Σ_2 and $\mathbf{P}(\mathbf{F}(\mathbf{u})) \cdot \mathbf{n} = \mathbf{0}$ on the top boundary Σ_4 . We set the same material parameters values as in the three-dimensional (3D) example in [3], in particular, we use $E = 1440$ Pa and $\nu = 0.25$. Figure 3(c) shows the displacement magnitude of the global solution \mathbf{u} in Ω . The reader can observe that the BCs applied have caused the domain to stretch by 1 m in the x direction.

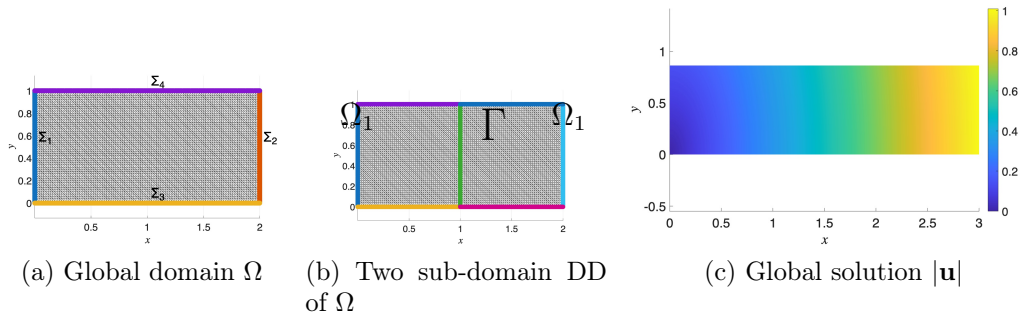


Figure 3: 2D nonlinear elasticity. (a) The global domain. (b) The global displacement magnitude solution. (c) Non-overlapping partition with $N_{\text{dd}} = 2$.

In studying the performance of the non-overlapping Schwarz alternating method, the global domain Ω is decomposed into two non-overlapping sub-domains discretized with uniform triangular meshes comprised of 10201 nodes, as shown in Figure 3(b). The characteristic measure of the finite element size h is set to 0.1 for both the global mesh and the sub-meshes. While the Schwarz alternating method is capable of coupling sub-domains having different meshes and mesh resolutions, we leave this use case to a future work. In applying the non-overlapping Schwarz alternating method, we specify the following algorithmic parameters: $\epsilon_{\text{abs}} = \epsilon_{\text{rel}} = 10^{-6}$, $\text{maxit} = 100$, and $\mathbf{g}^{(1)} = \mathbf{0}$. For the Newton nonlinear solver, we use a tolerance of 10^{-8} .

Remark 9. For nonlinear PDEs such as the one considered here, each non-linear sub-problem within the Schwarz algorithm requires an initial guess for the solution $\mathbf{u}_i^{(k)}$ at each Schwarz iteration k . While performing numerical

studies on the 2D nonlinear elasticity problem, we discovered that the Newton solver performance can be improved by: (i) solving a linear variant of the problem on-the-fly at each Schwarz iteration as a pre-processing step, and (ii) using the solutions to this linear problem as initial guesses for the Newton algorithm.

We define the following error metric to assess the accuracy of the DD methods

$$e_{max}(i) := \max \left(\sqrt{(u_{i,x} - u_x|_{\Omega_i})^2 + (u_{i,y} - u_y|_{\Omega_i})^2} \right). \quad (23)$$

Here, $\mathbf{u}_i : \Omega_i \rightarrow \mathbb{R}^2$ denotes the numerical sub-solution in Ω_i , where $\mathbf{u}_i = [u_{i,x}, u_{i,y}]^T$, with $u_{i,x}$ and $u_{i,y}$ denoting the horizontal and vertical components of the displacement, respectively. We denote by $\mathbf{u}|_{\Omega_i} : \Omega_i \rightarrow \mathbb{R}^2$ the restriction of the global solution to sub-domain Ω_i , where $\mathbf{u}|_{\Omega_i} = [u_x, u_y]^T = \mathbf{u}(\mathbf{x}) \forall \mathbf{x} \in \Omega_i$. While it is common to study the accuracy and convergence of numerical methods using relative, rather than absolute errors, the displacement solution to the 2D nonlinear elasticity problem is within the range $[0, 1]$, so that an absolute error is a reasonable metric to utilize.

3.2.1. Schwarz with classical relaxation

We begin by studying the convergence of the non-overlapping Schwarz alternating method accelerated using the classical relaxation scheme (Algorithm 1). In Figure 4, we depict the absolute and relative errors with respect to the Schwarz iteration k and for different values of the relaxation parameter $\rho \in \{0.1, 0.2, 0.3, 0.4, 0.5\}$. For $\rho > 0.5$, the algorithm did not converge. The reader can observe by examining Figure 4 that an intermediate value of $\rho = 0.4$ gives rise to convergence in the fewest number of Schwarz iterations.

3.2.2. Schwarz with Aitken acceleration

Next, we study convergence of the non-overlapping Schwarz alternating method with Aitken acceleration. Figures 5(a) and (b) show the Schwarz absolute and relative errors as a function of the Schwarz iteration k for different values of $\rho^{(1)}$. We only depict results for $\rho^{(1)} \in \{0.1, 0.2, 0.3, 0.4, 0.5\}$ since the algorithm did not converge for $\rho^{(1)} > 0.5$. We show results for two different values of the hyperparameter N_0 : $N_0 = 10$ (Figure 5(c)) and $N_0 = 2$ (Figure 5(d)). We remind the reader that, to the best of our knowledge, the

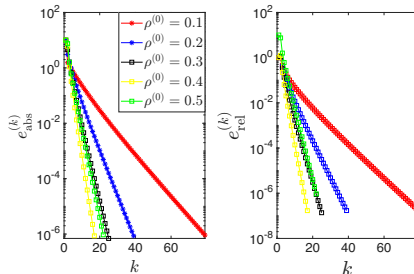


Figure 4: 2D nonlinear elasticity with $N_{\text{dd}} = 2$. Convergence of the Dirichlet-Neumann Schwarz alternating method with classical relaxation for different values of ρ . The left panel is showing convergence of $e_{\text{abs}}^{(k)}$, whereas the right panel shows convergence of $e_{\text{rel}}^{(k)}$.

introduction of the N_0 parameter into the Aitken scheme is new to this work. Comparing these figures with Figures 4(a) and (b), we conclude that, as expected, the Schwarz algorithm with a dynamical update of the relaxation parameter converges in a smaller number of iterations. We additionally observe that Aitken-accelerated Schwarz appears to be stable and robust with respect to different choices of the initial relaxation parameter $\rho^{(1)}$. Figure 5 suggests that, for the 2D nonlinear elasticity problem with $N_{\text{dd}} = 2$, selecting a smaller value of N_0 results in a smaller number of Schwarz iterations for a fixed value of $\rho^{(1)}$, though the algorithm is not particularly sensitive to the value of this parameter. Curiously, when we tried the smallest possible value, $N_0 = 1$, the method diverged.

Finally, in Figures 5(c)–(d), we depict the values of $\rho^{(k)}$ as a function of the Schwarz iteration k for $N_0 = 10$ and $N_0 = 2$. For $\rho^{(1)} < 0.5$, the optimal values of $\rho^{(k)}$ follow similar trends for $k > N_0$ and are generally larger than $\rho^{(1)}$.

3.2.3. Schwarz with classical Anderson acceleration

We now apply Anderson-accelerated Schwarz (Algorithm 4) to our 2D nonlinear elasticity problem with $N_{\text{dd}} = 2$. Note that, in this subsection, we are *not* considering the Anderson with memory adaptation approach described in Section 2.4.6. We use the same algorithmic settings as in the previous sections. For the solution of the constrained minimization problem (13), we opt for the quadratic programming function `quadprog` in MATLAB. We consider both the unrelaxed and relaxed versions of Anderson acceleration.

In Figure 6, we depict the $\alpha_i^{(k)}$ coefficients calculated in the Anderson op-

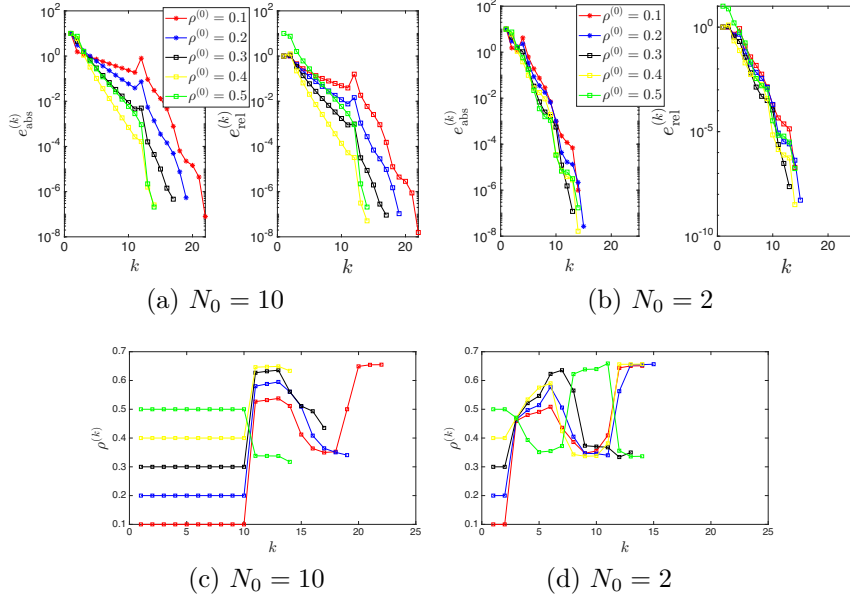


Figure 5: 2D nonlinear elasticity with $N_{\text{dd}} = 2$. Sub-plots (a) and (b) depict the convergence of Aitken-accelerated Schwarz for five different choices of $\rho^{(1)}$ and two choices of N_0 . Sub-plots (c) and (d) depict the values of the Aitken parameter $\rho^{(k)}$ as a function of the Schwarz iteration k , again for two choice of N_0 . The parameter N_0 is set to 10 in subfigures (a) and (c), and to 2 in subfigures (b) and (d).

timization procedure, which solves the constrained minimization problem (13). For a given m_{and} , the asymptotic value of $\alpha_i^{(k)}$ is $\approx \frac{1}{m_{\text{and}}+1}$ for all $i = 1, \dots, m_{\text{and}} + 1$, a result consistent with Theorem 2. We further notice that, while the $\alpha_i^{(k)}$ coefficients are not guaranteed to be between 0 and 1 (cf. Remark 8), they generally stay within this range.

In Figures 7(a) and (b), the norm of the residual $\|\mathbf{f}_k\|_2$ is depicted as a function of the Schwarz iteration number k . Unlike Schwarz with classical relaxation and Aitken-accelerated Schwarz, the reader can observe that Anderson-accelerated Schwarz is convergent for $\rho > 0.5$, including the $\rho = 1$ (unrelaxed) case; however, there is some sensitivity to the $m_{\text{and}} = 1$ parameter: in the case of $m_{\text{and}} = 1$ and larger values of ρ , the convergence is much slower, requiring almost the maximum amount `maxiter` of iterations. We additionally observe that oscillations in the residual norm (c.f., Figure 7(a)) may appear when utilizing unrelaxed Anderson-accelerated Schwarz.

One can additionally infer from Figures 7(a) and (b) that, for a fixed ρ ,

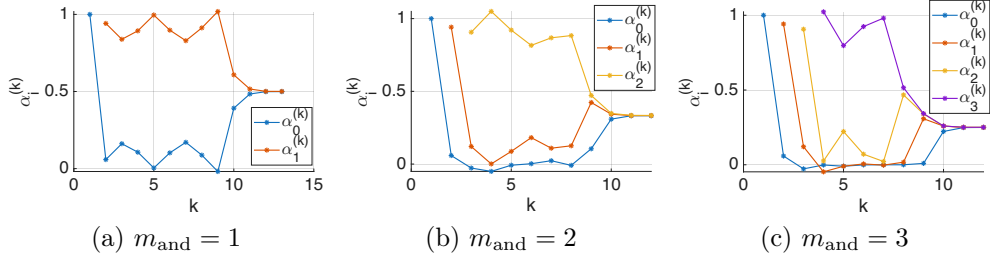


Figure 6: 2D nonlinear elasticity with $N_{\text{dd}} = 2$. Anderson coefficients $\alpha_i^{(k)}$ for $\rho = 0.5$ and increasing values of $m_{\text{and}} \in \{1, 2, 3\}$.

including more history information, i.e., using a larger value of m_{and} , can reduce the number of Schwarz iterations required for convergence; however this is true only up to a point. As shown in Figure 7(c), employing substantially larger values of m_{and} , e.g., $m_{\text{and}} = 20$ or higher while setting $m_{\text{and}} = k$, actually makes convergence worse. This result is consistent with the literature: as remarked in [24], if m_{and} is small, the secant information used by the method may be too limited to provide decidedly fast convergence, whereas if m_{and} is too large, the least-squares optimization problem for the α coefficients (13) may be poorly conditioned. While we did not observe stagnation in the Schwarz method’s convergence Figure 7 clearly shows that values of m_{and} on the order of 20 or greater lead to slow convergence and hence large compute times.

3.2.4. Schwarz accelerated using Anderson acceleration with memory adaptation

The results above motivated the construction of the “Anderson with memory adaptation” method described earlier in Section 2.4.6. We set a threshold of $\epsilon_{\text{and}} = 10^{-5}$ for the interface error $|e_{\text{rel}}^{(k)} - e_{\text{rel}}^{(k-1)}|$ and $\bar{m} = 3$. In Figure 8, we compare the convergence history of Anderson-accelerated Schwarz both with and without memory adaptation, with filled symbols denoting the classical Anderson method with a fixed m_{and} and empty symbols denoting Anderson with memory adaptation. In the sub-panel in Figure 8, we depict also the m_k values utilized by the Anderson with memory adaptation method, calculated according to the chosen criterion (20).

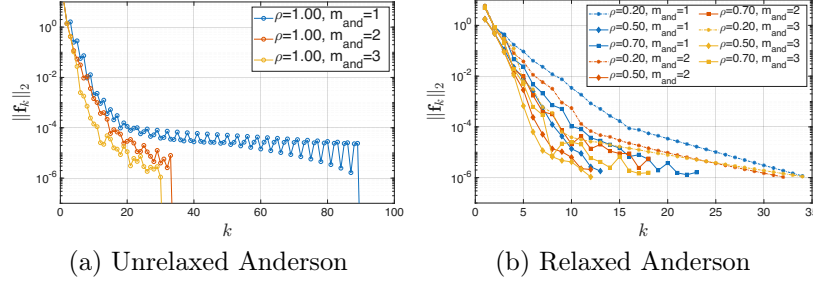


Figure 7: 2D nonlinear elasticity with $N_{\text{dd}} = 2$. Convergence of Anderson-accelerated Schwarz (without memory adaptation) for different values of ρ and m_{and} .

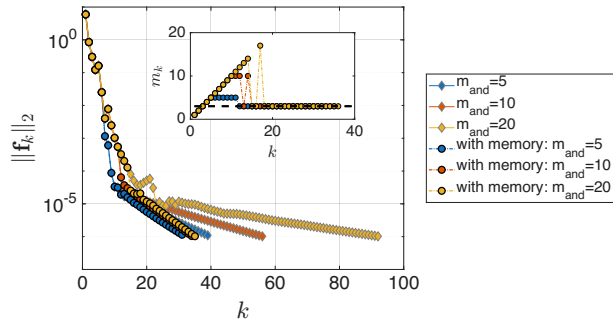


Figure 8: 2D nonlinear elasticity with $N_{\text{dd}} = 2$. Anderson with memory adaptation compared to the standard non-adapted Anderson with $\rho = 0.2$. In the sub-plot, the values of m_k chosen by the Anderson with memory technique are reported. The threshold in black represents $\bar{m} = 3$ for the condition in (20).

3.2.5. Methods comparison

In Table 3, we compare Anderson-accelerated Schwarz with no memory adaptation for $m_{\text{and}} = 1, 2, 3$ with the same algorithm accelerated using classical relaxation and Aitken acceleration in terms of errors with respect to the global solution for $\rho = \rho^{(1)} = 0.2$. Table 4 shows analogous results for the case $\rho = \rho^{(1)} = 0.5$. The following conclusions from Tables 3–4 are noteworthy: (i) Aitken-accelerated Schwarz is far less sensitive to $\rho^{(1)}$ than classically relaxed and Anderson-accelerated Schwarz are to ρ , (ii) the fastest convergence is achieved for Anderson-accelerated Schwarz with $\rho = 0.5$ and $m_{\text{and}} \in \{2, 3\}$ (Table 4), and (iii) while Aitken-accelerated Schwarz takes 1–2 more Schwarz iterations to converge than the “optimal” version of Anderson-accelerated Schwarz, it achieves a smaller value of the error $e_{\text{max}}(i)$ upon convergence.

	Classical relaxation	Aitken acceleration ($N_0 = 2$)	Anderson acceleration		
			$m_{\text{and}} = 1$	$m_{\text{and}} = 2$	$m_{\text{and}} = 3$
$e_{\text{max}}(1)$	5.06×10^{-7}	1.23×10^{-9}	1.49×10^{-7}	2.24×10^{-7}	3.96×10^{-7}
$e_{\text{max}}(2)$	2.58×10^{-7}	1.94×10^{-9}	7.61×10^{-8}	1.15×10^{-7}	2.04×10^{-7}
k	39	15	35	33	35

Table 3: 2D nonlinear elasticity with $N_{\text{dd}} = 2$. Accuracy and convergence comparisons between non-overlapping Schwarz with classical relaxation, and with the two acceleration methods evaluated. All methods evaluated used $\rho = \rho^{(1)} = 0.2$.

In Figure 9, we compare the relaxation/acceleration methods described so far in terms of relative error until convergence (or until the termination criterion on the maximum number of iterations). In Figure 9, we show the

	Classical relaxation	Aitken acceleration ($N_0 = 2$)	Anderson acceleration		
			$m_{\text{and}} = 1$	$m_{\text{and}} = 2$	$m_{\text{and}} = 3$
$e_{\text{max}}(1)$	5.78×10^{-7}	1.21×10^{-9}	1.38×10^{-7}	2.08×10^{-7}	2.34×10^{-7}
$e_{\text{max}}(2)$	1.14×10^{-7}	1.14×10^{-9}	2.12×10^{-7}	2.98×10^{-7}	1.83×10^{-7}
k	22	14	14	13	13

Table 4: 2D nonlinear elasticity with $N_{\text{dd}} = 2$. Accuracy and convergence comparisons between Schwarz with classical relaxation, and with the two acceleration methods evaluated. All methods evaluated used $\rho = \rho^{(1)} = 0.5$.

Schwarz convergence error in the case of different relaxation/acceleration techniques with $\rho = \rho^{(1)} = 0.2$ (Figure 9(a)) and $\rho = \rho^{(1)} = 0.5$ (Figure 9(b)). We do not report the unrelaxed Schwarz scheme for comparison, because, in this case, the algorithm does not converge. The plots in Figure 9 show that Aitken- and Anderson-accelerated Schwarz is more robust to the choice of $\rho = \rho^{(1)}$ than Schwarz with classical relaxation. This result is not surprising for the Aitken-accelerated version of the method, as the Aitken acceleration approach determines on-the-fly the optimal value of $\rho^{(k)}$ for $k > N_0$, rather than setting it to an *a priori*-specified constant value, as in classical relaxation and Anderson acceleration. The reader can observe that Anderson-accelerated Schwarz is not particularly sensitive to m_{and} .

An additional property which can be inferred from Figure 9 is the convergence rate. We numerically computed the convergence rate for the case $\rho = \rho^{(1)} = 0.5$ by calculating $C_k = \frac{|e_{\text{rel}}^{(k+1)}|}{|e_{\text{rel}}^k|^2}$, excluding the pre-asymptotic regime and the last iteration. Whereas the Schwarz alternating method with classical relaxation is converging at a linear or sub-linear rate ($C_k \in [0.3, 1]$), both Aitken- and Anderson-accelerated Schwarz converge at a rate that is almost quadratic ($C_k \in [0.5, 1.4]$). Additional comments on the computational

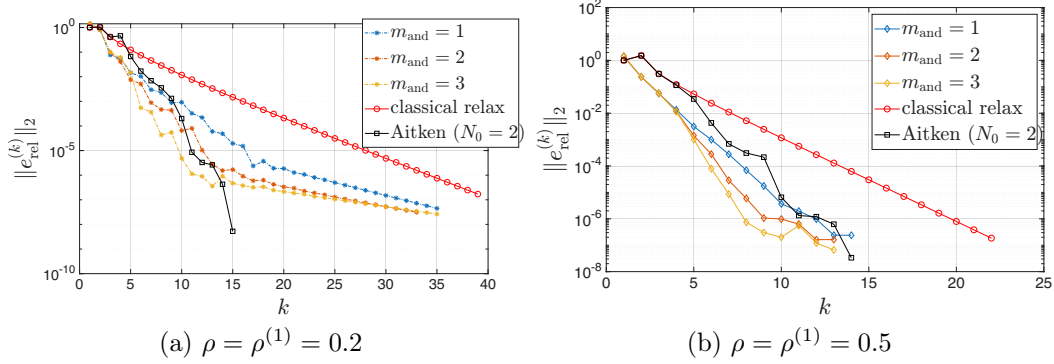


Figure 9: 2D nonlinear elasticity with $N_{\text{dd}} = 2$. Convergence of Schwarz with classical relaxation, Aitken acceleration and Anderson acceleration, with (a) $\rho = \rho^{(1)} = 0.2$, and (b) $\rho = \rho^{(1)} = 0.5$.

costs associated with all the techniques evaluated are postponed to the next section, where we consider the more general case of $N_{\text{dd}} \geq 2$.

3.2.6. A multi-domain study

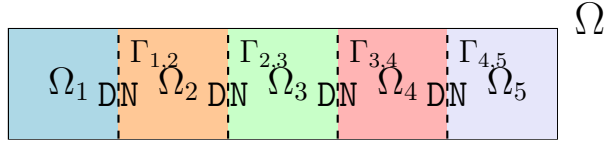


Figure 10: 2D nonlinear elasticity. Illustration of non-overlapping DD with $N_{\text{dd}} = 5$.

In the discussion above, we have limited our attention to the Schwarz alternating method applied to two non-overlapping sub-domains. Since the method typically requires more iterations to reach convergence when it is used to couple more sub-domains, there is a lot of interest in accelerating Schwarz when $N_{\text{dd}} > 2$. Toward this effect, we consider here the same 2D nonlinear elasticity problem studied earlier, but with a linear-in- x decomposition of our domain Ω into N_{dd} sub-domains, with $N_{\text{dd}} \in \{2, \dots, 5\}$. An example decomposition with $N_{\text{dd}} = 5$ is shown in Figure 10. The letters D and N in this figure indicate whether a Dirichlet or Neumann BC is specified on a given boundary as seen from sub-domain Ω_i during the Schwarz iteration procedure, with $i \in \{1, \dots, 5\}$. As before, we assess and compare the performance of the Schwarz alternating method with: (i) classical relax-

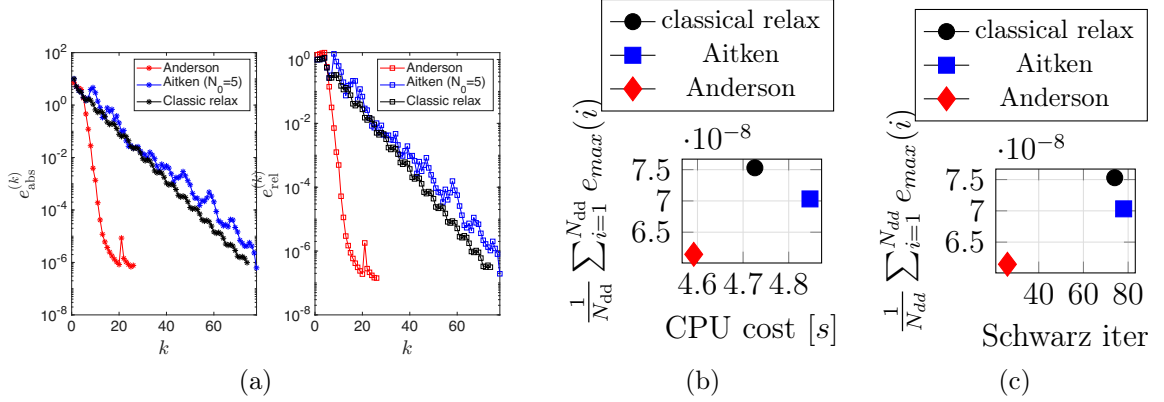


Figure 11: 2D nonlinear elasticity with $N_{dd} = 5$. Method comparison metrics with $\rho = 0.5$. (a) Schwarz convergence metrics $\epsilon_{abs}^{(k)}$ and $\epsilon_{rel}^{(k)}$ as a function of the Schwarz iteration k . (b) Average sub-domain error $e_{max}(i)$ as a function of the average per iteration CPU time (in seconds). (c) Average sub-domain error $e_{max}(i)$ as a function of the number of Schwarz iterations required to reach convergence.

ation, (ii) Aitken acceleration with $N_0 = 5$ and $\rho^{(1)} = 0.5$, and (iii) Anderson acceleration with memory adaptation based on $m_{and} = 20$, $\epsilon_{and} = 10^{-5}$ and $\bar{m} = 3$. The multi-domain implementation of Aitken acceleration is a natural extension of the procedure described in Section 2.4 to the multi-domain setting, in which the Aitken acceleration procedure is applied to each set of neighboring sub-domains independently. The approach is based on the assumption that the inverse Jacobian $\mathbf{G}^{(k)}$ in (17) is constant for all the sub-domains $i = 1, \dots, N_{dd}$, and corresponds to the Aitken variant termed the ‘‘Diagonal Aitken’’ technique in [23]. In all our studies, we used a value of $\text{maxit} = 80$ for the maximum allowable number of Schwarz iterations. We employed Anderson with memory adaptation, as it reduced the number of iterations required to reach convergence by a factor of three with respect to the standard Anderson method with a fixed m_k .

Figures 11(a)–(c) study the convergence and performance of the Dirichlet-Neumann Schwarz algorithm with the different acceleration techniques considered for $N_{dd} = 5$. The reader can observe that Anderson-accelerated Schwarz is the clear winner in terms of not only the number of Schwarz iterations required to reach convergence (Figures 11(a) and (c)), but also in terms of the CPU time per Schwarz iteration (Figure 11(b)). Generally, Anderson-accelerated Schwarz converges in approximately $3\times$ fewer itera-

tions than Aitken-accelerated Schwarz. Curiously, the convergence of Aitken-accelerated Schwarz is actually worse than that of Schwarz with classical relaxation. These results differ from our previously-reported results for the specific case of $N_{\text{dd}} = 2$, which showed that Aitken-accelerated Schwarz often outperforms, or performs comparably to, Anderson-accelerated Schwarz (see Tables 3–4 and Figure 9). The poor convergence of Aitken-accelerated Schwarz is consistent with previously-reported results [23], which showed non-convergence of this algorithm for $N_{\text{dd}} > 2$ when applied to a fluid-structure interaction problem. It is somewhat surprising that Anderson-accelerated Schwarz has the lowest CPU time per Schwarz iteration (Figure 11(b)), as it is the only method that requires the online numerical solution of an optimization problem. This result is likely due to the fast optimized algorithms within the `quadrprog` MATLAB routine, which we use to solve the Anderson minimization problem. It is interesting to remark that the Schwarz alternating method accelerated using Anderson with memory adaptation exhibited some sensitivity to the m_{and} parameter. In particular, setting m_{and} to a smaller value resulted in more iterations required to reach convergence. For example, with $m_{\text{and}} = 5$, the method converged in 54 iterations, whereas it converged in just 26 iterations for $m_{\text{and}} = 20$.

We performed additional tests using two other values of the Aitken acceleration parameter: $\rho^{(1)} = 0.2$ and $\rho^{(1)} = 0.7$. For these choices, the Aitken acceleration approach negatively affects the performance of the local Newton solver and prevents the Schwarz algorithm from converging. In contrast, Anderson-accelerated Schwarz appears to be more robust with respect to the choice of ρ , converging in 60 and 29 iterations for $\rho = 0.2$ and $\rho = 0.7$, respectively.

Remark 10. There are more sophisticated variants of the Aitken algorithm, e.g., the “Block Aitken” [23] and the sparse Aitken-Schwarz methods [26]. These and other variants of Aitken-accelerated Schwarz may be studied in a future work.

Finally, we analyze how the performance and scalability of Schwarz with our various acceleration techniques depends on the number of sub-domains. In Figure 12, we present both the average of the per-iteration CPU time (Figure 12(a)), and the number of total Schwarz iterations needed to achieve convergence (Figure 12(b)) for $N_{\text{dd}} \in \{2, \dots, 5\}$. We observe that the number of Schwarz iterations required for convergence for Aitken-accelerated Schwarz scales roughly linearly with N_{dd} ; in contrast, Anderson-accelerated Schwarz

appears to be much more robust to increases in N_{dd} (Figure 12(b)). Again, we see that Anderson-accelerated Schwarz does not require a significantly higher CPU costs than the other two techniques (Figure 12(a)).

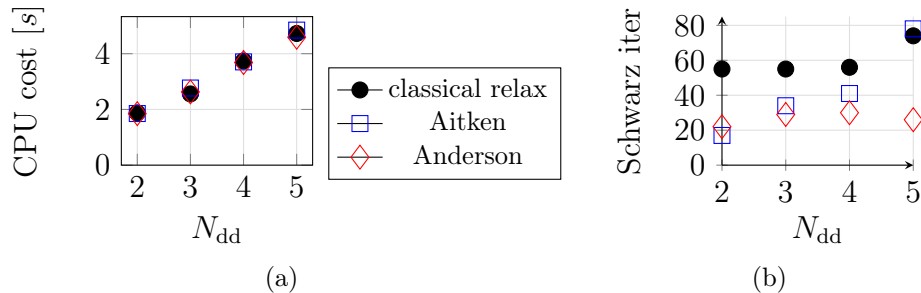


Figure 12: 2D nonlinear elasticity with $N_{\text{dd}} \in \{2, 3, 4, 5\}$. (a) N_{dd} vs. the average CPU time (in seconds) per Schwarz iteration. (b) N_{dd} vs. the number of Schwarz iterations required to reach convergence.

4. Conclusions and perspectives

In this work, we have presented a theoretical and numerical comparison of the impact of various relaxation and acceleration techniques on the convergence of the multiplicative Schwarz alternating method with Dirichlet-Neumann transmission conditions in the context of DD-based coupling and elliptic BVPs. For a 1D model problem, we proved quadratic convergence of Aitken-accelerated Schwarz under some conditions, and uncovered a link between the spectral properties of the underlying fixed-point operator and the Anderson acceleration coefficients in Anderson-accelerated Schwarz. We compared both theoretically and numerically the various acceleration techniques on a simple linear PDE, the 1D Laplace equation. We also studied the methods' accuracy, performance and robustness (to both algorithmic parameters and the number of sub-domains being coupled) on a 2D nonlinear elasticity problem. For the two sub-domain setting, we demonstrated that the convergence of Aitken-accelerated Schwarz is not particularly sensitive to the two tuning parameters in this algorithm, $\rho^{(1)}$ and N_0 , which makes the algorithm appealing to users as minimal parameter tuning/optimization is required. We also demonstrated that the method can be twice as fast as Anderson-accelerated Schwarz and Schwarz with classical relaxation. The story is different when considering greater numbers of sub-domains, where

Anderson-accelerated Schwarz is the most performant and robust method, requiring $4\times$ fewer iterations to converge than the other methods evaluated. We discovered that, while Anderson-accelerated Schwarz has a larger memory footprint, its computational cost is approximately equal to Aitken-accelerated Schwarz and Schwarz with classical relaxation. Our observation that Anderson-accelerated Schwarz can be sensitive to its input parameter m_{and} , which controls the size of the history utilized within the Anderson update formula, led to the development of a new adaptive version of Anderson, termed “Anderson with memory adaptation”, which leads to a more robust and performant Schwarz scheme.

The research summarized in this work has informed several directions for future work, which include: (i) numerical investigations of the accelerated methods’ performance on problems with sub-domains discretized using non-conformal meshes, (ii) explorations of different variants of Aitken-accelerated Schwarz for the multi-domain scenario (e.g., the “Block Aitken” method in [23]), (iii) reformulations of the Anderson update formula such that the relaxation parameter ρ is updated dynamically rather than pre-specified, (iv) extensions to 3D and time-dependent problems, and (v) the development of acceleration strategies for the Robin-Robin version of the non-overlapping Schwarz alternating method.

Appendix A. Derivation of the Aitken acceleration formula (9)

To show that the Aitken acceleration formula (9) is obtained when minimizing the function (10), we follow the procedure in Section 4.2.3 of [23]. In Section 2.3, we wrote the Dirichlet-Neumann Schwarz algorithm as a fixed-point iteration (c.f., equation (5e)). To simplify the notation here, we consider conforming interfaces, so that $\gamma = \gamma_1 = \gamma_2$ and $\Pi_{12} = \Pi_{21} = \mathbb{I}$. The sub-domain interface jump (8) also simplifies to $\mathcal{E}(\gamma(\mathbf{u}_1), \gamma(\mathbf{u}_2)) = \gamma(\mathbf{u}_2) - \gamma(\mathbf{u}_1)$. The fixed-point iteration reads $\mathbf{g}^* = T(\mathbf{g}^*)$ if and only if $\mathcal{E}(\gamma(\mathbf{u}_1^*), \gamma(\mathbf{u}_2^*)) = \mathbf{0}$, with \mathbf{u}_1^* and \mathbf{u}_2^* the solution to the Dirichlet and Neumann problems once \mathbf{g}^* is given. We denote by $\tilde{\rho}$ the approximation of the inverse of Jacobian function with respect to the discrepancy. Following [23], we approximate the inverse of the Jacobian by a scalar time the identity, i.e. $\tilde{\rho} = -\rho\mathbb{I}$. Now, if we apply Newton’s method, we obtain, for $k > 0$,

$$\begin{aligned}\gamma(\mathbf{u}_1^{*,(k-1)}) &= \gamma(\mathbf{u}_1^{(k-1)}) - \tilde{\rho}\mathcal{E}(\gamma(\mathbf{u}_1^{(k-1)}), \gamma(\mathbf{u}_2^{(k-1)})) \\ \gamma(\mathbf{u}_1^{*,(k)}) &= \gamma(\mathbf{u}_1^{(k)}) - \tilde{\rho}\mathcal{E}(\gamma(\mathbf{u}_1^{(k)}), \gamma(\mathbf{u}_2^{(k)}))\end{aligned}\tag{A.1a}$$

at iteration $k - 1$ and k . Since system (A.1a) is not well-defined, we employ a least-squares technique to find the optimal ρ :

$$\begin{aligned}
\rho^{(k)} &= \arg \min_{\rho \in \mathbb{R}} \left\| \gamma(\mathbf{u}_1^{*,(k)}) - \gamma(\mathbf{u}_1^{*,(k-1)}) \right\|_2^2 \\
&= \arg \min_{\rho \in \mathbb{R}} \left\| \underbrace{\left(\gamma(\mathbf{u}_1^{(k)}) - \gamma(\mathbf{u}_1^{(k-1)}) \right)}_{\mathbf{d}^{(k)}} + \rho \underbrace{\left(\mathcal{E}\left(\gamma(\mathbf{u}_1^{(k)}), \gamma(\mathbf{u}_2^{(k)})\right) - \mathcal{E}\left(\gamma(\mathbf{u}_1^{(k-1)}), \gamma(\mathbf{u}_2^{(k-1)})\right) \right)}_{\boldsymbol{\delta}^{(k)}} \right\|_2^2 \\
&= \arg \min_{\rho \in \mathbb{R}} \left\| \mathbf{d}^{(k)} + \rho \boldsymbol{\delta}^{(k)} \right\|_2^2.
\end{aligned}$$

It is easy to see that the solution is (9).

Acknowledgments

Support for this work was received through Sandia National Laboratories' (SNL's) Laboratory Directed Research and Development (LDRD) program, as well as through the U.S. Department of Energy (DOE), Office of Science, Office of Advanced Scientific Computing Research Mathematical Multifaceted Integrated Capability Centers (MMICCs) program (under Field Work Proposal 22025291 and the Multifaceted Mathematics for Predictive Digital Twins project) and Applied Mathematics Competitive Portfolios program. Additionally, the writing of this manuscript was funded in part by I. Tezaur's Presidential Early Career Award for Scientists and Engineers (PECASE). The corresponding author gratefully acknowledges support from the SIAM Postdoctoral Support Program fellowship. SNL is a multi-mission laboratory managed and operated by National Technology and Engineering Solutions of Sandia, LLC., a wholly owned subsidiary of Honeywell International, Inc., for the U.S. DOE's National Nuclear Security Administration under contract DE-NA0003525.

The authors also thank Dr. Tommaso Taddei for his helpful comments on an earlier version of this work.

References

- [1] V. Dolean, P. Jolivet, F. Nataf, An introduction to domain decomposition methods: algorithms, theory, and parallel implementation, SIAM, 2015.

- [2] M. J. Gander, et al., Schwarz methods over the course of time 31 (5) (2008) 228–255.
- [3] A. Mota, I. Tezaur, C. Alleman, The Schwarz alternating method in solid mechanics 319 (2017) 19–51.
- [4] A. Mota, I. Tezaur, G. Phlipot, The Schwarz alternating method for dynamic solid mechanics, *International Journal for Numerical Methods in Engineering* (2022) 1–36 [doi:10.1002/nme.6982](https://doi.org/10.1002/nme.6982).
- [5] J. Barnett, I. Tezaur, A. Mota, The schwarz alternating method for the seamless coupling of nonlinear reduced order models and full order models (2022).
- [6] C. R. Wentland, F. Rizzi, J. L. Barnett, I. K. Tezaur, The role of interface boundary conditions and sampling strategies for Schwarz-based coupling of projection-based reduced order models 465 (2025) 116584.
- [7] C. Rodriguez, I. Tezaur, A. Mota, A. Gruber, E. Parish, C. Wentland, Transmission conditions for the non-overlapping Schwarz coupling of full order and Operator Inference models, *arXiv preprint arXiv:2509.12228* (2025).
- [8] I. Tezaur, E. Parish, A. Gruber, I. Moore, C. Wentland, A. Mota, Hybrid coupling with operator inference and the overlapping Schwarz alternating method (2026). [arXiv:2511.20687](https://arxiv.org/abs/2511.20687).
- [9] I. Moore, C. Wentland, A. Gruber, I. Tezaur, Domain decomposition-based coupling of Operator Inference reduced order models via the Schwarz alternating method (2024). [arXiv:2409.01433](https://arxiv.org/abs/2409.01433).
- [10] H. Schwarz, Uber einen grenzübergang durch alternierendes verfahren, *Vierteljahrsschrift der Naturforschenden Gesellschaft in Zurich* 15 (1870) 272–286.
- [11] S. Sobolev, Schwarz’s Algorithm in Elasticity Theory, in: G. Demidenko, V. Vaskevich (Eds.), *Selected Works of S.L Sobolev. Volume I: Equations of Mathematical Physics, Computational Mathematics and Cubature Formulas*, Springer, New York, 2006.

- [12] S. Mikhlin, On the Schwarz algorithm, Proceedings of the USSR Academy of Sciences (in Russian) 77 (1951) 569–571.
- [13] P.-L. Lions, et al., On the Schwarz alternating method. I, in: 1st international symposium on domain PDEs, Vol. 1, Paris, France, 1988, p. 42.
- [14] P. Lions, On the Schwarz alternating method III: A variant for nonoverlapping subdomains, in 3rd International Symposium on Domain Decomposition Methods for PDEs, T. F. Chan, R. Glowinski, J. Periaux, and O. B. Widlund, eds., SIAM (1990).
- [15] P. Zanolli, Domain decomposition algorithms for spectral methods 24 (3) (1987) 201–240.
- [16] D. Funaro, A. Quarteroni, P. Zanolli, An iterative procedure with interface relaxation for domain decomposition methods 25 (6) (1988) 1213–1236.
- [17] F. Kwok, Neumann-Neumann waveform relaxation for the time-dependent heat equation, in: Domain Decomposition Methods in Science & Engineering XXI, Springer, 2014, pp. 189–198.
- [18] B. C. Mandal, Neumann–neumann waveform relaxation algorithm in multiple subdomains for hyperbolic problems in 1d and 2d, Numerical Methods for Partial Differential Equations 33 (2) (2017) 514–530.
- [19] M. J. Gander, F. Kwok, B. C. Mandal, [Dirichlet-Neumann and Neumann-Neumann waveform relaxation algorithms for parabolic problems](#) (2014). [arXiv:1311.2709](#).
URL <https://arxiv.org/abs/1311.2709>
- [20] M. J. Gander, O. Dubois, Optimized schwarz methods for a diffusion problem with discontinuous coefficient, Numerical Algorithms 69 (1) (2015) 109–144.
- [21] A. Toselli, O. Widlund, Domain decomposition methods-algorithms and theory, Vol. 34, Springer Science & Business Media, 2004.

- [22] J. Côté, M. J. Gander, L. Laayouni, S. Loisel, Comparison of the Dirichlet-Neumann and optimal Schwarz method on the sphere, in: Domain Decomposition Methods in Science & Engineering, Springer, 2005, pp. 235–242.
- [23] S. Deparis, Numerical analysis of axisymmetric flows and methods for fluid-structure interaction arising in blood flow simulation, Ph.D. thesis, Verlag nicht ermittelbar (2004).
- [24] H. F. Walker, P. Ni, Anderson acceleration for fixed-point iterations, SIAM Journal on Numerical Analysis 49 (4) (2011) 1715–1735.
- [25] M. Garbey, D. Tromeur-Dervout, On some Aitken-like acceleration of the Schwarz method, International Journal for Numerical Methods in Fluids 40 (12) (2002) 1493–1513. [doi:10.1002/flid.407](https://doi.org/10.1002/flid.407).
- [26] L. Berenguer, D. Tromeur-Dervout, Sparse Aitken–Schwarz domain decomposition with application to Darcy flow, Computers & Fluids 249 (2022) 105687. [doi:https://doi.org/10.1016/j.compfluid.2022.105687](https://doi.org/10.1016/j.compfluid.2022.105687).
- [27] S. Deparis, M. Discacciati, A. Quarteroni, A domain decomposition framework for fluid-structure interaction problems, in: CFD 2004: Proceedings of the 3rd International Conference on CFD, ICCFD3, Toronto, 12–16 July 2004, Springer, 2006, pp. 41–58.
- [28] A. Mota, D. Koliesnikova, I. Tezaur, J. Hoy, A fundamentally new coupled approach to contact mechanics via the Dirichlet-Neumann Schwarz alternating method, International Journal for Numerical Methods in Engineering 126 (9) (2025) e70039.
- [29] E. Zappon, A. Manzoni, P. Gervasio, A. Quarteroni, A reduced order model for domain decompositions with non-conforming interfaces, Journal of Scientific Computing 99 (1) (2024) 22.
- [30] A. Quarteroni, A. Valli, Domain Decomposition Methods for Partial Differential Equations, Oxford University Press, Oxford, UK, 1999.
- [31] A. Toselli, O. B. Widlund, Domain Decomposition Methods – Algorithms and Theory, Vol. 34 of Lecture Notes in Computational Science and Engineering, Springer, Berlin / Heidelberg, 2005.

- [32] L. D. Marini, A. Quarteroni, A relaxation procedure for domain decomposition methods using finite elements 55 (5) (1989) 575–598.
- [33] A. Quarteroni, A. Valli, Domain decomposition methods for partial differential equations, Oxford University Press, 1999.
- [34] B. F. Smith, P. E. Bjørstad, W. D. Gropp, Domain Decomposition: Parallel Multilevel Methods for Elliptic PDEs, Cambridge University Press, Cambridge, UK, 1996.
- [35] N. Discacciati, J. S. Hesthaven, Model reduction of coupled systems based on non-intrusive approximations of the boundary response maps, Computer Methods in Applied Mechanics and Engineering 420 (2024) 116770. [doi:10.1016/j.cma.2024.116770](https://doi.org/10.1016/j.cma.2024.116770).
- [36] A. Toth, C. T. Kelley, Convergence analysis for Anderson acceleration, SIAM Journal on Numerical Analysis 53 (2) (2015) 805–819.
- [37] A. Mota, J. A. Zimmerman, A variational, finite-deformation constitutive model for piezoelectric materials, International Journal for Numerical Methods in Engineering 85 (6) (2011) 752–767. [doi:10.1002/nme.2993](https://doi.org/10.1002/nme.2993).